

# Braneflamagnetogenesis from cosmoparticle physics after Planck

Sayantana Choudhury<sup>a</sup>

<sup>a</sup>Department of Theoretical Physics, Tata Institute of Fundamental Research, Colaba, Mumbai - 400005, India <sup>1</sup>

E-mail: [sayantana@theory.tifr.res.in](mailto:sayantana@theory.tifr.res.in)

**Abstract.** In this article, I have studied the cosmoparticle constraints on a generic class of large field ( $|\Delta\phi| > M_p$ ) and small field ( $|\Delta\phi| < M_p$ ) models of brane inflationary magnetogenesis *aka* “braneflamagnetogenesis” from: (1) tensor-to-scalar ratio ( $r$ ), (2) reheating, (3) leptogenesis and (4) baryogenesis in case of Randall-Sundrum single braneworld gravity (RSII) framework. I also establish a direct connection between the magnetic field at the present epoch ( $B_0$ ) and primordial gravity waves ( $r$ ), which give a precise estimate of non-vanishing CP asymmetry ( $\epsilon_{CP}$ ) in leptogenesis and baryon asymmetry ( $\eta_B$ ) in baryogenesis scenario respectively. Further assuming the conformal invariance to be restored after inflation in the framework of RSII, I have explicitly shown that the requirement of the sub-dominant feature of large scale coherent magnetic field after inflation gives two fold non-trivial characteristic constraints- on equation of state parameter ( $w$ ) and the corresponding energy scale during reheating ( $\rho_{rh}^{1/4}$ ) epoch. Hence giving the proposal for avoiding the contribution of back-reaction from the magnetic field I have established a bound on the generic reheating characteristic parameter ( $R_{rh}$ ) and its rescaled version ( $R_{sc}$ ), to achieve large scale magnetic field within the prescribed setup and further apply the CMB constraints as obtained from recently observed Planck 2015 data and Planck+BICEP2+Keck Array joint constraints. Using all these derived results I have shown that it is possible to put further stringent constraints on various classes of large and small field inflationary models to break the degeneracy between various cosmophenomenological parameters within the framework of RSII. Finally, I have studied the consequences from two specific models of brane inflation- monomial and hilltop, after applying all the constraints obtained from “braneflamagnetogenesis”.

---

<sup>1</sup>Presently working as a Visiting (Post-Doctoral) fellow at DTP, TIFR, Mumbai, Alternative E-mail: [sayanphysicsisi@gmail.com](mailto:sayanphysicsisi@gmail.com).

---

## Contents

<b>1</b>	<b>Introduction</b>	<b>1</b>
<b>2</b>	<b>Parametrization of magnetic power spectrum</b>	<b>3</b>
<b>3</b>	<b>Constraint on inflamagnetogenesis from leptogenesis and baryogenesis</b>	<b>6</b>
<b>4</b>	<b>Braneinflamagnetogenesis via reheating</b>	<b>14</b>
4.1	Basic assumptions	14
4.2	Reheating parameter	15
4.3	Evading magnetic back-reaction	16
<b>5</b>	<b>Reheating constraints on braneinflamagnetogenesis</b>	<b>18</b>
<b>6</b>	<b>Constraining models of braneinflamagnetogenesis from CMB</b>	<b>22</b>
6.1	Monomial Models	23
6.2	Hilltop Models	35
<b>7</b>	<b>Summary</b>	<b>46</b>
<b>8</b>	<b>Appendix</b>	<b>48</b>
8.1	Inflationary consistency relations in RSII	48
8.2	Evaluation of $I_\xi(k_L, k_\Lambda)$ integral kernel	50
8.3	Evaluation of $J(k_L, k_\Lambda)$ integral kernel	50

---

## 1 Introduction

Large scale magnetic fields are ubiquitously present across the entire universe. They are a major component of the interstellar medium e.g. stars, galaxies and galactic clusters of galaxies<sup>1</sup>. It has been verified by different astronomical observations, but their true origin is a big mystery of cosmology and astro-particle physics [3–6]. The generation mechanism and the limits of the magnetic fields within the range  $\mathcal{O}(5 \times 10^{-17} - 10^{-14})$  Gauss [7] in the intergalactic medium have been recently studied using combined constraints from the Atmospheric Cherenkov Telescopes and the Fermi Gamma-Ray Space Telescope on the spectra of distant blazars. The upper bound on primordial magnetic fields could be also obtained from the cosmic microwave background (CMB) and the large scale structure (LSS) observations, and the current upper bound is given by  $\mathcal{O}(10^{-9})$  Gauss from Faraday rotations [8] and the lower bound is fixed at  $\mathcal{O}(10^{-15})$

---

<sup>1</sup>Magnetic fields in galaxies have a strength ,  $\mathcal{O}(5 \times 10^{-6} - 10^{-4})$  Gauss [1] and the detected strength within clusters of galaxies is,  $\mathcal{O}(10^{-6} - 10^{-5})$  Gauss [2].

Gauss by HESS and Fermi/LAT observations [9–11]. If the magnetic fields are produced in the early universe, then they mimic the role of seed for the observed galactic and cluster magnetic field, as well as directly explain the origin of the magnetic fields present at the interstellar medium. Among various possibilities “inflationary magnetogenesis” aka “inframagnetogenesis” is one of the plausible mechanism, through which the generation of cosmic magnetic field generation at the early universe can widely be explained. Within the prescription of “inframagnetogenesis”, large scale coherent magnetic fields and the primordial curvature perturbations are generated from the quantum fluctuations. However the generation of cosmic magnetic field via “inframagnetogenesis” is not possible in an elementary fashion as in the context of standard electromagnetic theory the action <sup>2</sup>:

$$S = \int d^4x \sqrt{-g} g^{\alpha\mu} g^{\beta\nu} F_{\mu\nu} F_{\alpha\beta} \quad (1.1)$$

is conformally invariant. Consequently in FLRW cosmological background for a co-moving observer  $u_\nu$  the magnetic field:

$$B^\mu = -\frac{1}{2} \epsilon^{\mu\nu\alpha\beta} u_\nu F_{\alpha\beta} = -{}^* F^{\mu\nu} u_\nu \quad (1.2)$$

always decrease with the scale factor in an inverse square manner and implies the rapid decay of magnetic field during inflation. In a flat universe, this issue can be resolved by breaking the conformal invariance of the electromagnetic theory during inflationary epoch <sup>3</sup>. See refs. [12–25] for the further details of this issue. Due to the breaking of conformal invariance of the electromagnetic theory the magnetic field gets amplified. On the other hand, during inflation the back-reaction effect of the electromagnetic field spoils the underlying picture. Also the theoretical origin and the specific technical details of the conformal invariance breaking mechanism makes the back-reaction effect model dependent. However, in this paper, during the analysis it is assumed that after the end of inflation conformal invariance is restored in absence of source and the magnetic field decreases with the scale factor in an inverse square fashion. Also by suppressing the effect of back-reaction after inflation, in this work, I derive various useful constraints on- reheating, leptogenesis and baryogenesis in a model independent way.

---

<sup>2</sup> In Eq (1.1),  $F_{\mu\nu}$  is the electromagnetic field strength tensor and is defined as,  $F_{\mu\nu} = \partial_{[\mu} A_{\nu]}$ , where  $A_\mu$  is the  $U(1)$  gauge field.

<sup>3</sup> One of the simplest, gauge invariant model of “inframagnetogenesis” is described by the following effective action [12, 13]:

$$S = \int d^4x \sqrt{-g} f^2(\phi) g^{\alpha\mu} g^{\beta\nu} F_{\mu\nu} F_{\alpha\beta} \quad (1.3)$$

where the conformal invariance of the  $U(1)$  gauge field  $A_\mu$  is broken by a time dependent function  $f(\phi) (\propto a^\alpha)$  of inflaton  $\phi$  and at the end of inflation  $f(\phi_{end}) \rightarrow 1$ .

The prime objective of this paper to establish a theoretical constraint for a generic class of large field ( $|\Delta\phi| > M_p$ <sup>4</sup>) and small field ( $|\Delta\phi| < M_p$ ) model of inflationary magnetogenesis in the framework of Randall-Sundrum braneworld gravity (RSII) [26–34, 37–40] *aka* “braneinflationmagnetogenesis” from various probes: (1) tensor-to-scalar ratio ( $r$ ), (2) reheating, (3) leptogenesis [41, 42, 57] and (4) baryogenesis [44–47]. The plan of the paper is as follows. In the section 3, I will explicitly show that for all of these generic class of inflationary models it is possible to predict the amount of magnetic field at the present epoch ( $B_0$ ), by measuring non-vanishing CP asymmetry ( $\epsilon_{CP}$ ) in leptogenesis and baryon asymmetry ( $\eta_B$ ) in baryogenesis or the tensor-to-scalar ratio. In this paper I use various constraints arising from Planck 2015 data on the amplitude of scalar power spectrum, scalar spectral tilt, the upper bound on tensor to scalar ratio, lower bound on rescaled characteristic reheating parameter and the bound on the reheating energy density within  $1.5\sigma - 2\sigma$  statistical CL. I also mention the GR limiting result and the difference between the high energy limit result of RSII. Further assuming the conformal invariance to be restored after inflation in the framework of Randall-Sundrum single braneworld gravity (RSII), I will show that the requirement of the sub-dominant feature of large scale magnetic field after inflation gives two fold non-trivial characteristic constraints- on equation of state parameter ( $w$ ) and the corresponding energy scale during reheating ( $\rho_{rh}^{1/4}$ ) epoch in section 3. Hence in section 4 and 5 avoiding the contribution of back-reaction from the magnetic field I have established a bound on the reheating characteristic parameter ( $R_{rh}$ ) and its rescaled version ( $R_{sc}$ ), to achieve large scale magnetic field within the prescribed setup and apply the Cosmic Microwave Background (CMB) constraints as obtained from recent Planck 2015 data [48–50] and the joint constraint obtained from Planck+BICEP2+Keck Array [51]. Finally in section 6, I will explicitly study the cosmophenomenological consequences from two specific models of brane inflation- monomial (large field) and hilltop (small field) after applying all the constraints obtained in this paper. Moreover, by doing parameter estimation from both of these simple class of models, I will explicitly show the magneto-reheating constraints can be treated as one of the probes through which one can distinguish between the prediction from both of these inflationary models.

## 2 Parametrization of magnetic power spectrum

A Gaussian random magnetic field for a statistically homogeneous and isotropic system is described by the equal time two-point correlation function in momentum space as [52, 53]:

$$\langle B_i^*(\mathbf{k}, \eta) B_j(\mathbf{k}', \eta) \rangle = (2\pi)^3 \delta^{(3)}(\mathbf{k} - \mathbf{k}') \mathcal{P}_{ij}(\hat{\mathbf{k}}) P_{\mathbf{B}}(k), \quad (2.1)$$

---

<sup>4</sup>Field excursion of the inflation field is defined as:  $\Delta\phi = \phi_{cmb} - \phi_{end}$ , where  $\phi_{cmb}$  represent the field value of the inflaton at the momentum scale  $k$  which satisfies the equality,  $k = aH = -\eta^{-1} \approx k_*$ , where ( $a$ ,  $H$ ,  $\eta$ ) represent the scale factor, Hubble parameter, the conformal time and pivot momentum scale respectively. Also  $\phi_{end}$  is the field value of the inflaton defined at the end of inflation.

where the plane projector onto the transverse plane is defined as [52, 53]:

$$\mathcal{P}_{ij}(\hat{\mathbf{k}}) = \sum_{\lambda=\pm 1} e_i^\lambda(\hat{\mathbf{k}}) e_j^{-\lambda}(\hat{\mathbf{k}}) = (\delta_{ij} - \hat{\mathbf{k}}_i \hat{\mathbf{k}}_j) \quad (2.2)$$

in which the divergence-free nature of the magnetic field is imposed via the orthogonality condition,  $\hat{\mathbf{k}}^i \epsilon_i^{\pm 1} = 0$ . Here  $\hat{\mathbf{k}}_i$  signifies the unit vector which can be expanded in terms of spin spherical harmonics. See ref. [52] for the details of the useful properties of the projection tensors of magnetic modes. Additionally, it is worthwhile to mention that in the present context,  $P_{\mathbf{B}}(k)$  be the part of the power spectrum for the primordial magnetic field which will only contribute to the cosmological perturbations for the scalar modes and the Faraday Rotation at the phase of decoupling<sup>5</sup>.

The non-helical part of the primordial magnetic power spectrum is parameterized within the upper and lower cut-off momentum scale ( $k_L \leq k \leq k_\Lambda$ ) as [54]:

$$P_{\mathbf{B}}(k) = \begin{cases} A_{\mathbf{B}} & \text{for Case I} \\ A_{\mathbf{B}} \left( \frac{k}{k_*} \right)^{n_{\mathbf{B}}} & \text{for Case II} \\ A_{\mathbf{B}} \left( \frac{k}{k_*} \right)^{n_{\mathbf{B}} + \frac{\alpha_{\mathbf{B}}}{2} \ln\left(\frac{k}{k_*}\right)} & \text{for Case III} \\ A_{\mathbf{B}} \left( \frac{k}{k_*} \right)^{n_{\mathbf{B}} + \frac{\alpha_{\mathbf{B}}}{2} \ln\left(\frac{k}{k_*}\right) + \frac{\kappa_{\mathbf{B}}}{6} \ln^2\left(\frac{k}{k_*}\right)} & \text{for Case IV} \end{cases} \quad (2.3)$$

where  $A_{\mathbf{B}}$  represents amplitude of the magnetic power spectrum,  $n_{\mathbf{B}}$  is the magnetic spectral tilt,  $\alpha_{\mathbf{B}}$  is the running and  $\kappa_{\mathbf{B}}$  be the running of the magnetic spectral tilt. Here the upper cut-off momentum scale ( $k_\Lambda$ ) corresponds to the Alfvén wave damping length-scale, representing the dissipation of magnetic energy due to the generation of magneto-hydrodynamic (MHD) waves. Additionally,  $k_*$  being the pivot or normalization scale of momentum. Now let me briefly discuss the physical significance of the above mentioned four possibilities:

- **Case I** stands for a physical situation where the magnetic power spectrum is exactly scale invariant,
- **Case II** stands for a physical situation where the magnetic power spectrum follows power law feature in presence of magnetic spectral tilt  $n_{\mathbf{B}}$ ,
- **Case III** signifies a physical situation where the magnetic power spectrum shows deviation from power law behaviour in presence of running of the magnetic spectral tilt  $\alpha_{\mathbf{B}}$  along with logarithmic correction in the momentum scale (as appearing in the exponent) and

---

<sup>5</sup>It is important to mention here that, the exact form of the magnetic power power spectrum strongly depends on the production mechanism of primordial magnetic field.

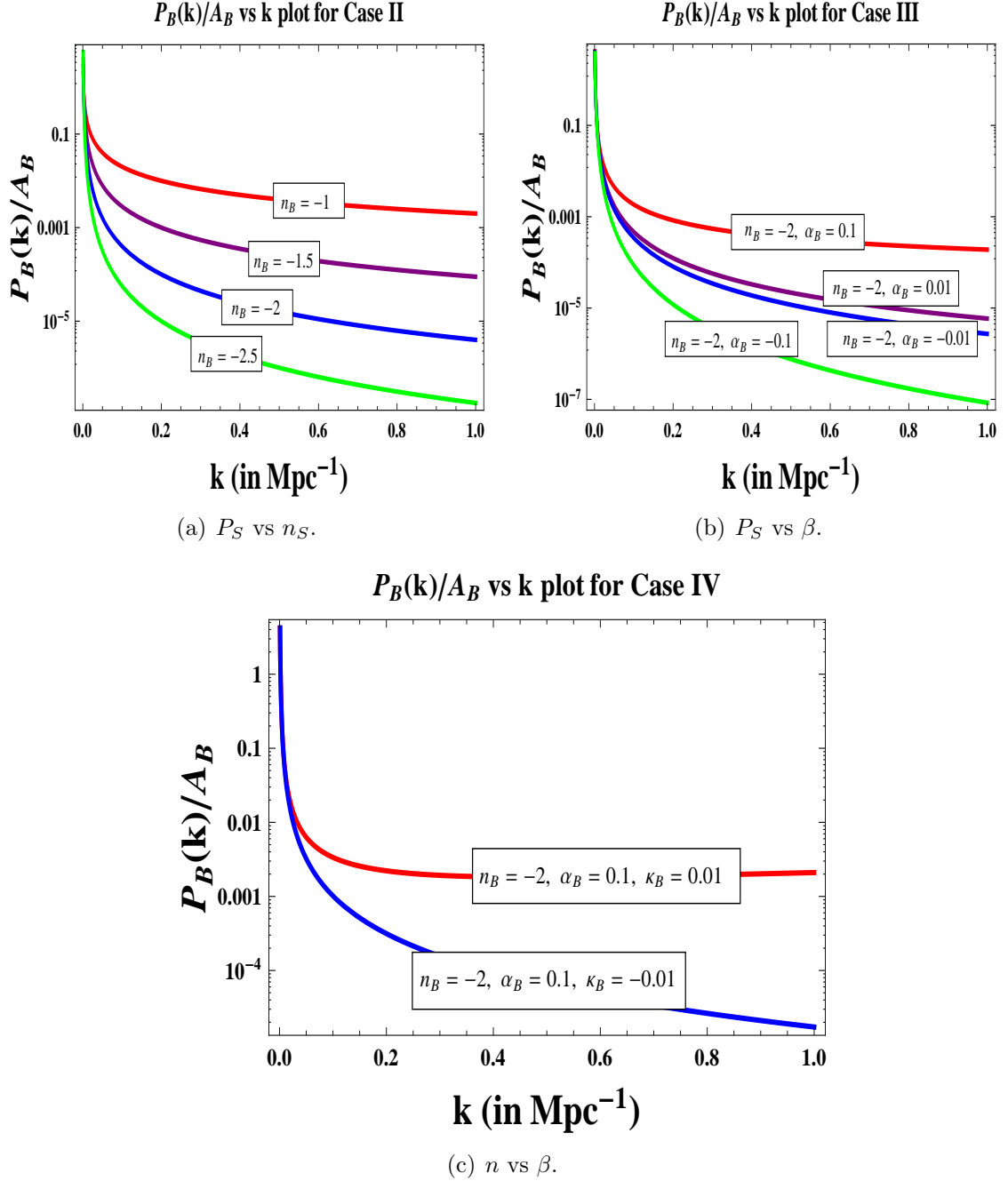


**Figure 1.** Variation of the magnetic power spectrum with respect to momentum scale  $k$  for **1(a)**  $n_B < 0, \alpha_B = 0, \kappa_B = 0$ , **1(b)**  $n_B < 0, \alpha_B \neq 0, \kappa_B = 0$  and **1(c)**  $n_B < 0, \alpha_B \neq 0, \kappa_B \neq 0$ .

- **Case IV** characterizes a physical situation in which the magnetic power spectrum is further modified compared to the **Case III**, by allowing running of the running of the magnetic spectral tilt  $\kappa_B$  along with square of the momentum dependent logarithmic correction.

In fig. **1(a)**-fig. **1(c)** I have explicitly shown the variation of the magnetic power spec-

trum with respect to momentum scale  $k$  for  $n_{\mathbf{B}} < 0, \alpha_{\mathbf{B}} = 0, \kappa_{\mathbf{B}} = 0$ ,  $n_{\mathbf{B}} < 0, \alpha_{\mathbf{B}} \neq 0, \kappa_{\mathbf{B}} = 0$  and  $n_{\mathbf{B}} < 0, \alpha_{\mathbf{B}} \neq 0, \kappa_{\mathbf{B}} \neq 0$  respectively. It is important to note that the most recent observational constraint from CMB temperature anisotropies on the amplitude and the spectral index of a primordial magnetic field has been predicted by using Planck 2015 data as  $B_{1 \text{ Mpc}} < 4.4 \text{ nG}$  <sup>6</sup> with  $n_{\mathbf{B}} < 0$  at  $2\sigma$  CL [48, 49]. If, in near future, Planck or any other observational probes can predict the signatures for  $\alpha_{\mathbf{B}}$  and  $\kappa_{\mathbf{B}}$  in the primordial magnetic power spectrum (as already predicted in case of primordial scalar power spectrum within  $1.5 - 2\sigma$  CL [50]), then it is possible to put further stringent constraint on the various models of inflation.

### 3 Constraint on inflamagnetogenesis from leptogenesis and baryogenesis

In the present section, I am interested in the mean square amplitude of the primordial magnetic field on a given characteristic scale  $\xi$ , on which I smooth the magnetic power spectrum using a Gaussian filter <sup>7</sup> as given by [53]:

$$B_{\xi}^2 = \langle B_i(\mathbf{x}) B_i(\mathbf{x}) \rangle_{\xi} = \frac{1}{2\pi^2} \int_0^{\infty} \frac{dk}{k_*} \left( \frac{k}{k_*} \right)^2 P_{\mathbf{B}}(k) \exp(-k^2 \xi^2). \quad (3.1)$$

Here in Case III and Case IV of Eq (2.3) describes a more generic picture where the magnetic power spectrum deviates from its exact power law form in presence of logarithmic correction. Consequently, the resulting mean square primordial magnetic field is logarithmically divergent in both the limits of the integral as presented in Eq (3.1). But in Case I and Case II of Eq (2.3) no such divergence is appearing. To remove the divergent contribution from the mean square amplitude of the primordial magnetic field as appearing in Case III and Case IV of Eq (3.1), I introduce here cut-off regularization technique in which I have re-parameterized the integral in terms of regulated UV (high) and IR (low) momentum scales. Most importantly, for the sake of completeness for all four cases, here I introduce the high and low cut-offs  $k_{\Lambda}$  and  $k_L$  are momentum regulators to collect only the finite contributions from Eq (3.1). Finally I get:

$$B_{\xi}^2(k_L; k_{\Lambda}) = \frac{I_{\xi}(k_L; k_{\Lambda})}{2\pi^2} A_{\mathbf{B}} \quad (3.2)$$

---

<sup>6</sup>Here  $B_{1 \text{ Mpc}}$  represents the comoving field amplitude at a scale of 1 Mpc.

<sup>7</sup>In standard prescriptions, Gaussian filter is characterized by a Gaussian window function  $\exp(-k^2 \xi^2)$ , defined in a characteristic scale  $\xi$ .

where

$$I_\xi(k_L; k_\Lambda) = \begin{cases} \int_{k_L}^{k_\Lambda} \frac{dk}{k_*} \exp(-k^2 \xi^2) \left(\frac{k}{k_*}\right)^2 & \text{for Case I} \\ \int_{k_L}^{k_\Lambda} \frac{dk}{k_*} \exp(-k^2 \xi^2) \left(\frac{k}{k_*}\right)^{n_{\mathbf{B}}+2} & \text{for Case II} \\ \int_{k_L}^{k_\Lambda} \frac{dk}{k_*} \exp(-k^2 \xi^2) \left(\frac{k}{k_*}\right)^{n_{\mathbf{B}}+2+\frac{\alpha_{\mathbf{B}}}{2} \ln\left(\frac{k}{k_*}\right)} & \text{for Case III} \\ \int_{k_L}^{k_\Lambda} \frac{dk}{k_*} \exp(-k^2 \xi^2) \left(\frac{k}{k_*}\right)^{n_{\mathbf{B}}+2+\frac{\alpha_{\mathbf{B}}}{2} \ln\left(\frac{k}{k_*}\right)+\frac{\kappa_{\mathbf{B}}}{6} \ln^2\left(\frac{k}{k_*}\right)} & \text{for Case IV.} \end{cases} \quad (3.3)$$

The exact expression for the regularized integral function  $I_\xi(k_L; k_\Lambda)$  are explicitly mentioned in the appendix 8.1 for all four cases. it is important to mention here that, for Case I and Case II,  $I_\xi(k_L \rightarrow 0; k_\Lambda \rightarrow \infty)$  is finite. But for rest of the two cases,  $I_\xi(k_L \rightarrow 0; k_\Lambda \rightarrow \infty) \rightarrow \infty$ . On the other hand, in absence of any Gaussian filter, the magnetic energy density can be expressed in terms of the mean square primordial magnetic field as [53]:

$$\rho_{\mathbf{B}} = \frac{1}{8\pi} \langle B_i(\mathbf{x}) B_i(\mathbf{x}) \rangle = \frac{1}{8\pi^2} \int_0^\infty \frac{dk}{k_*} \left(\frac{k}{k_*}\right)^2 P_{\mathbf{B}}(k) \quad (3.4)$$

which is logarithmically divergent in UV and IR end for Case III and Case IV. For rest of the two cases also the contribution become divergent, but the behaviour of the divergences are different compared to the Case III and Case IV. After introducing the momentum cut-offs as mentioned earlier, I get the regularized expression for the magnetic energy density as:

$$\rho_{\mathbf{B}}(k_L; k_\Lambda) = \frac{J(k_L; k_\Lambda)}{8\pi^2} A_{\mathbf{B}} = \frac{J(k_L; k_\Lambda) B_\xi^2(k_L; k_\Lambda)}{4I_\xi(k_L; k_\Lambda)} \quad (3.5)$$

where

$$J(k_L; k_\Lambda) = \begin{cases} \int_{k_L}^{k_\Lambda} \frac{dk}{k_*} \left(\frac{k}{k_*}\right)^2 & \text{for Case I} \\ \int_{k_L}^{k_\Lambda} \frac{dk}{k_*} \left(\frac{k}{k_*}\right)^{n_{\mathbf{B}}+2} & \text{for Case II} \\ \int_{k_L}^{k_\Lambda} \frac{dk}{k_*} \left(\frac{k}{k_*}\right)^{n_{\mathbf{B}}+2+\frac{\alpha_{\mathbf{B}}}{2} \ln\left(\frac{k}{k_*}\right)} & \text{for Case III} \\ \int_{k_L}^{k_\Lambda} \frac{dk}{k_*} \left(\frac{k}{k_*}\right)^{n_{\mathbf{B}}+2+\frac{\alpha_{\mathbf{B}}}{2} \ln\left(\frac{k}{k_*}\right)+\frac{\kappa_{\mathbf{B}}}{6} \ln^2\left(\frac{k}{k_*}\right)} & \text{for Case IV} \end{cases} \quad (3.6)$$

where I use Eq (3.2). Here the regularized integral function  $J(k_L; k_\Lambda)$  are explicitly written in the appendix 8.2 for all four possibilities.



Now to derive a phenomenological constraint here I further assume the fact that the primordial magnetic field is made up of relativistic degrees of freedom. In this physical prescription, the regularized magnetic energy density can be expressed as [55]:

$$\rho_{\mathbf{B}}(k_L; k_\Lambda) \sim \frac{\pi^2}{30} g_* T^4 \sim \mathcal{O}(10^{-13}) \times \frac{T^4}{\epsilon_{\mathbf{CP}}} \quad (3.7)$$

where the CP asymmetry parameter  $\epsilon_{\mathbf{CP}}$  is defined as:

$$\epsilon_{\mathbf{CP}} = \frac{\Gamma_L(N_R \rightarrow L_i \Phi) - \Gamma_{L^c}(N_R \rightarrow L_i^c \Phi^c)}{\Gamma_L(N_R \rightarrow L_i \Phi) + \Gamma_{L^c}(N_R \rightarrow L_i^c \Phi^c)} \approx \mathcal{O}(|\lambda|^2) \sin \theta_{\mathbf{CP}} \quad (3.8)$$

for the standard leptogenesis scenario [56, 57] where the Majorana neutrino ( $N_R$ ) decays through Yukawa matrix interaction ( $\lambda$ ) with the Higgs ( $\Phi$ ) and lepton ( $L$ ) doublets. Here where  $\theta_{\mathbf{CP}}$  is the CP-violating phase and for heavy majorana neutrino ( $N_R$ ) mass  $10^{10} \text{ GeV}$  the Yukawa coupling is given by,  $|\lambda|^2 = \mathcal{O}(10^{-16})$ . Now combining Eq (3.5) and Eq (3.7) I derive the following simplified expression for the root mean square value of the primordial magnetic field at the present epoch in terms of the CP asymmetry parameter ( $\epsilon_{\mathbf{CP}}$ ) as:

$$B_0 \sim \mathcal{O}(10^{-14}) \times \sqrt{\frac{I_\xi(k_L = k_0; k_\Lambda)}{J(k_L = k_0; k_\Lambda) \epsilon_{\mathbf{CP}}}} \text{ Gauss} \quad (3.9)$$

where I use the temperature at the present epoch  $T_0 \sim 2 \times 10^{-4} \text{ eV}$  and  $1 \text{ Gauss} = 7 \times 10^{-20} \text{ GeV}^2$ . In addition, here in this paper, I fix the IR cut-off scale of the momentum at the present epoch i.e.  $k_L = k_0$ . Consequently the momentum integrals satisfy the following constraint:

$$\sqrt{\frac{I_\xi(k_L = k_0; k_\Lambda)}{J(k_L = k_0; k_\Lambda)}} \sim 10^{-8}. \quad (3.10)$$

Further using Eq (8.16) and Eq (8.17) in Eq 3.10 one can write the following constarints for all four cases of the parametrization of magnetic power spectrum as:

$$\textbf{Case I :} \quad k_* \sim \mathcal{O}(8.17 \times 10^{-9}) \times \sqrt{\frac{\sqrt{\xi} [k_\Lambda^3 - k_L^3]}{\sqrt{\pi} [\text{erf}(\xi k_\Lambda) - \text{erf}(\xi k_L)]}}, \quad (3.11)$$

$$\textbf{Case II :} \quad \frac{1}{\xi^{n_B+3}} \sim \mathcal{O}(2 \times 10^{-16}) \times \frac{[k_\Lambda^{n_B+3} - k_L^{n_B+3}]}{(n_B + 3) \left[ \Gamma\left(\frac{(n_B+3)}{2}, \xi^2 k_L^2\right) - \Gamma\left(\frac{(n_B+3)}{2}, \xi^2 k_\Lambda^2\right) \right]}, \quad (3.12)$$

$$\begin{aligned}
\text{Case III : } & \left[ \frac{\sqrt{\pi} \operatorname{erf}(\xi k)}{2\xi} \left\{ 1 + \mathcal{Q} \ln \left( \frac{k}{k_*} \right) + \mathcal{P} \ln^2 \left( \frac{k}{k_*} \right) \right\} \right. \\
& + k \left\{ 2\mathcal{P} {}_P F_Q \left[ \left\{ \frac{1}{2}, \frac{1}{2}, \frac{1}{2} \right\} ; \left\{ \frac{3}{2}, \frac{3}{2}, \frac{3}{2} \right\} ; -\xi^2 k^2 \right] \right. \\
& \left. \left. - \left( \mathcal{Q} + 2\mathcal{P} \ln \left( \frac{k}{k_*} \right) \right) {}_P F_Q \left[ \left\{ \frac{1}{2}, \frac{1}{2} \right\} ; \left\{ \frac{3}{2}, \frac{3}{2} \right\} ; -\xi^2 k^2 \right] \right\} \right]_{k=k_L}^{k=k_\Lambda} \\
& \sim \mathcal{O}(10^{-16}) \times \left\{ k \left[ (1 + 2\mathcal{P} - \mathcal{Q}) + (\mathcal{Q} - 2\mathcal{P}) \ln \left( \frac{k}{k_*} \right) + \mathcal{P} \ln^2 \left( \frac{k}{k_*} \right) \right] \right\}_{k=k_L}^{k=k_\Lambda},
\end{aligned} \tag{3.13}$$

$$\begin{aligned}
\text{Case IV : } & \left[ \frac{\sqrt{\pi} \operatorname{erf}(\xi k)}{2\xi k_*} \left\{ 1 + \mathcal{Q} \ln \left( \frac{k}{k_*} \right) + \mathcal{P} \ln^2 \left( \frac{k}{k_*} \right) + \mathcal{F} \ln^3 \left( \frac{k}{k_*} \right) \right\} \right. \\
& + \left( \frac{k}{k_*} \right) \left\{ -6\mathcal{F} {}_P F_Q \left[ \left\{ \frac{1}{2}, \frac{1}{2}, \frac{1}{2}, \frac{1}{2} \right\} ; \left\{ \frac{3}{2}, \frac{3}{2}, \frac{3}{2}, \frac{3}{2} \right\} ; -\xi^2 k^2 \right] \right. \\
& + 2 \left( \mathcal{P} + 3\mathcal{F} \ln \left( \frac{k}{k_*} \right) \right) {}_P F_Q \left[ \left\{ \frac{1}{2}, \frac{1}{2}, \frac{1}{2} \right\} ; \left\{ \frac{3}{2}, \frac{3}{2}, \frac{3}{2} \right\} ; -\xi^2 k^2 \right] \\
& \left. \left. - \left( \mathcal{Q} + 2\mathcal{P} \ln \left( \frac{k}{k_*} \right) + 6\mathcal{F} \ln^2 \left( \frac{k}{k_*} \right) \right) \right. \right. \\
& \left. \left. \times {}_P F_Q \left[ \left\{ \frac{1}{2}, \frac{1}{2} \right\} ; \left\{ \frac{3}{2}, \frac{3}{2} \right\} ; -\xi^2 k^2 \right] \right\} \right]_{k=k_L}^{k=k_\Lambda} \\
& \sim \mathcal{O}(10^{-16}) \times \left\{ \left( \frac{k}{k_*} \right) \left[ (1 - 6\mathcal{F} + 2\mathcal{P} - \mathcal{Q}) + (6\mathcal{F} - 2\mathcal{P} + \mathcal{Q}) \ln \left( \frac{k}{k_*} \right) \right. \right. \\
& \left. \left. - (3\mathcal{F} - \mathcal{P}) \ln^2 \left( \frac{k}{k_*} \right) + \mathcal{F} \ln^3 \left( \frac{k}{k_*} \right) \right] \right\}_{k=k_L}^{k=k_\Lambda},
\end{aligned} \tag{3.14}$$

where  $\mathcal{Q} = n_B + 2$ ,  $\mathcal{P} = \alpha_B/2$  and  $\mathcal{F} = \kappa_B/6$ . The conformal symmetry of the quantized electromagnetic field breaks down in curved space-time which is able to generate a sizable amount of magnetic field during a phase of slow-roll inflation. Such primordial magnetism is characterized by the renormalized mean square amplitude of the primordial magnetic field at leading order in slow-roll approximation for comoving observers as [58]:

$$\rho_{\mathbf{B}}(k_L; k_\Lambda) = \frac{1}{8\pi} \langle B_i(\mathbf{x}) B_i(\mathbf{x}) \rangle \approx \frac{V^4(\phi) \epsilon_b(\phi)}{8640\pi^3 M_p^4 \sigma^2} \tag{3.15}$$

where  $V(\phi)$  represents the inflationary potential,  $\sigma$  represents the brane tension of RSII setup and  $M_p \sim 2.43 \times 10^{18}$  GeV be the four dimensional reduced Planck mass. Within RSII setup the visible brane tension  $\sigma$  can be expressed as [31]:

$$\sigma = \sqrt{-\frac{3}{4\pi} M_5^3 \Lambda_5} = \sqrt{-24 M_5^3 \tilde{\Lambda}_5} > 0 \tag{3.16}$$

where  $\tilde{\Lambda}_5$  be the scaled 5D bulk cosmological constant defined as [31]:

$$\tilde{\Lambda}_5 = \frac{\Lambda_5}{32\pi} < 0. \tag{3.17}$$

Also the 5D quantum gravity cut-off scale can be expressed in terms of 5D cosmological constant and the 4D effective Planck scale as:

$$M_5^3 = \sqrt[3]{-\frac{4\pi\Lambda_5}{3}} M_p^{4/3} = \sqrt[3]{-\frac{128\pi^2\tilde{\Lambda}_5}{3}} M_p^{4/3}. \quad (3.18)$$

In the high energy regime the energy density  $\rho \gg \sigma$  the slow-roll parameter  $\epsilon_b(\phi)$  in the visible brane can be expressed as [31]:

$$\epsilon_b(\phi) \approx \frac{2M_p^2\sigma(V'(\phi))^2}{V^3(\phi)}. \quad (3.19)$$

It is important to note that Eq (3.15) is insensitive to the intrinsic ambiguities of renormalization in curved space-times. See the appendix where I have mentioned the inflationary consistency conditions within RSII setup. Around the pivot scale  $k = k_*$  I can write:

$$\epsilon_b(k_*) \approx \frac{r(k_*)}{24} + \dots, \quad (3.20)$$

where  $\dots$  includes the all the higher order slow-roll contributions. Here  $r = P_T/P_S$  represents the tensor-to-scalar ratio. The recent observations from Planck (2013 and 2015) and Planck+BICEP2+Keck Array puts an upper bound on the amplitude of *primordial gravitational waves* via tensor-to-scalar ratio. This bounds the potential energy stored in the inflationary potential within RSII setup as [31]:

$$\begin{aligned} \sqrt[4]{V_{inf}} &\approx \sqrt[12]{2\pi^2 P_S(k_*)r(k_*)} M_p^{1/3} \sigma^{1/6} \lesssim \sqrt[4]{\frac{3}{2} P_S(k_*)r(k_*)\pi^2} M_p \\ &= (1.96 \times 10^{16} \text{GeV}) \times \left( \frac{r(k_*)}{0.12} \right)^{1/4} \end{aligned} \quad (3.21)$$

where  $P_S(k_*)$  represents the amplitude of the scalar power spectrum. More precisely Eq (3.21) can be recast as a stringent constraint on the upper bound on the brane tension in RSII setup during inflation as:

$$\sigma < \frac{3\sqrt{3}}{4} \pi^2 P_S(k_*) r(k_*) M_p^4. \quad (3.22)$$

It is important to note that, to validate the effective field theory prescription within the framework of small field models of inflation, the model independent bound on the brane tension, the 5D cut-off scale and 5D bulk cosmological constant can be written as [31]:

$$\sigma \leq \mathcal{O}(10^{-9}) M_p^4, \quad M_5 \leq \mathcal{O}(0.04 - 0.05) M_p, \quad \tilde{\Lambda}_5 \geq -\mathcal{O}(10^{-15}) M_p^5. \quad (3.23)$$

If we go beyond the above mentioned bound on the characteristic parameters of RSII then one can describe the inflationary paradigm in large field regime. Please see ref. [31] for further details.

Finally using this constraint along with Eq (3.5) in Eq (3.15) I get the following simplified expression for the root mean square value of the primordial magnetic field in terms of the tensor-to-scalar ratio  $r$  in RSII setup as <sup>8</sup>:

$$B_\xi(k_L; k_\Lambda) \lesssim \mathcal{O}(10^{35}) \times \left( \frac{r(k_*)}{0.12} \right)^{5/2} \underbrace{\Sigma_b^{5/2}(k_L, k_*) \times \left( \frac{M_p^4}{\sigma} \right)}_{\text{Regulator in RSII}} \times \sqrt{\frac{I_\xi(k_L; k_\Lambda)}{J(k_L; k_\Lambda)}} \text{ Gauss.} \quad (3.26)$$

At the present epoch the regulating factor  $\Sigma_b(k_L = k_0, k_*)$  appearing in Eq (3.26) is lying within the window,

$$\mathcal{O}(4.77 \times 10^{13}) \leq \Sigma_b(k_L = k_0, k_*) \times \left( \frac{M_p^4}{\sigma} \right)^{2/5} \leq \mathcal{O}(10^{-17.6}), \quad (3.27)$$

for the tensor-to-scalar ratio,  $10^{-29} \leq r_* \leq 0.12$  at the momentum pivot scale,  $k_* \sim 0.002 \text{ Mpc}^{-1}$ . Here the “b” subscript is used to specify the fact that the analysis is done within RSII setup. Now by setting  $k_L = k_0$  at the present epoch, the estimated numerical value of the primordial magnetic field from RSII setup turns out to be:

$$B_0 = B_\xi(k_L = k_0; k_\Lambda) \sim \mathcal{O}(10^{-9}) \text{ Gauss.} \quad (3.28)$$

Further using Eq (3.9) we get following expression for the lower bound of the CP asymmetry parameter within RSII setup as <sup>9</sup>:

$$\epsilon_{\text{CP}} \gtrsim \mathcal{O}(10^{-98}) \times \left( \frac{0.12}{r(k_*)} \right)^5 \Sigma_b^{-5}(k_L = k_0, k_*) \times \left( \frac{\sigma}{M_p^4} \right)^2, \quad (3.30)$$

which is pointing towards the following possibilities within RSII setup:

---

<sup>8</sup>In case of the low energy limit of RSII setup the Friedmann equations are mapped into the results for GR prescribes setup. In the low energy regime of RSII the lower bound of the CP asymmetry parameter can be written as [54]:

$$B_\xi(k_L; k_\Lambda) \lesssim \mathcal{O}(10^{44}) \times \left( \frac{r(k_*)}{0.12} \right)^{3/2} \underbrace{\Sigma^{3/2}(k_L, k_*)}_{\text{Regulator in GR}} \times \sqrt{\frac{I_\xi(k_L; k_\Lambda)}{J(k_L; k_\Lambda)}} \text{ Gauss.} \quad (3.24)$$

where  $\Sigma(k_L = k_0, k_*)$  plays the GR analogue of the regulator and satisfies the following stringent constraint:

$$\mathcal{O}(10^{-2/3}) \leq \Sigma(k_L = k_0, k_*) \leq \mathcal{O}(10^{-30}). \quad (3.25)$$

<sup>9</sup>In case of low energy regime of RSII or equivalently for GR prescribed setup the lower bound of the CP asymmetry parameter can be written as [54]:

$$\epsilon_{\text{CP}} \gtrsim \mathcal{O}(10^{-116}) \times \left( \frac{0.12}{r(k_*)} \right)^3 \Sigma^{-3}(k_L = k_0, k_*), \quad (3.29)$$

where  $\Sigma(k_L = k_0, k_*)$  plays the GR analogue of the regulator.

1. For the large tensor-to-scalar ratio the significant features of CP asymmetry can be possible to detect in future collider experiments. For an example we consider a situation where the tensor-to-scalar ratio is,  $r(k_*) \sim 0.12$  and in such a case the lower bound of CP asymmetry is given by  $\epsilon_{\mathbf{CP}} \gtrsim 10^{-10}$  in RSII braneworld. For GR one can also compute the lower bound of CP asymmetry parameter and it turns out to be  $\epsilon_{\mathbf{CP}} \gtrsim 10^{-16}$  for GR limit [54].
2. For very small tensor-to-scalar ratio the CP asymmetry is largely suppressed and can't be possible to detect in the particle colliders. For an example if tensor-to-scalar ratio,  $r(k_*) \sim 10^{-29}$  then the lower bound of CP asymmetry is given by  $\epsilon_{\mathbf{CP}} \gtrsim 10^{-26}$  in RSII braneworld. Similarly the lower bound of CP asymmetry parameter in GR prescribed setup can be computed as,  $\epsilon_{\mathbf{CP}} \gtrsim 10^{-30}$  [54].

If, in near future, any direct/indirect observational probe detects the signatures of primordial gravitational waves by measuring large detectable amount of tensor-to-scalar ratio then it will follow the first possibility. For a rough estimate for CP asymmetry in terms of neutrino masses one can write:

$$\epsilon_{\mathbf{CP}} \sim \frac{3}{16\pi} \frac{M_1 m_3}{v^2} \sim 0.1 \frac{M_1}{M_3}. \quad (3.31)$$

This implies that in the first case it is highly possible to achieve the upper bound of CP asymmetry parameter,  $\epsilon_{\mathbf{CP}} \lesssim 10^{-6}$  [54] for  $M_1/M_3 \sim m_u/m_t \sim 10^{-5}$ , by tuning the regulating factor as well the brane tension of RSII setup at the pivot scale  $k_* \sim 0.002 \text{ Mpc}^{-1}$  to the following value <sup>10</sup>:

$$\Sigma_b(k_L = k_0, k_*) \times \left( \frac{M_p^4}{\sigma} \right)^{2/5} \lesssim \mathcal{O}(4 \times 10^{-19}), \quad (3.33)$$

which is required to accommodate mass hierarchy of the heavy Majorana neutrino at the scale of  $10^{10} \text{ GeV}$ . Additionally it is important mention here that the heavy Majorana neutrino  $N_R$  is the ideal candidate for baryogenesis as decays to lepton-Higgs pairs yield lepton asymmetry  $\langle L \rangle_T \neq 0$ , partially converted to baryon asymmetry  $\langle B \rangle_T \neq 0$ . Also the baryon asymmetry  $\eta_B$  for given CP asymmetry  $\epsilon_{\mathbf{CP}}$  can be expressed as:

$$\eta_B = \frac{n_B - n_{\bar{B}}}{n_\gamma} = \frac{\kappa}{f} c_\Delta \epsilon_{\mathbf{CP}} \quad (3.34)$$

where  $f \sim 10^2$  is the dilution factor which accounts for the increase of the number of photons in a comoving volume element between baryogenesis and today,  $c_\Delta$  represents

---

<sup>10</sup>In case of low energy regime of RSII or equivalently for GR prescribed setup the upper bound on the tuning in the regulator can be expressed as:

$$\Sigma(k_L = k_0, k_*) \lesssim \mathcal{O}(2.1 \times 10^{-37}). \quad (3.32)$$

the fraction which is responsible for the conversion of lepton asymmetry to baryon asymmetry and exactly quantified by the following expression:

$$c_\Delta = \frac{\langle B \rangle_T}{\langle B - L \rangle_T} = \frac{1}{1 - \frac{\langle L \rangle_T}{\langle B \rangle_T}}. \quad (3.35)$$

Usually the conversion factor  $c_\Delta \sim \mathcal{O}(1)$  and in the context of Standard Model  $c_\Delta = 28/79$ . Also the determination of the washout factor  $\kappa$  requires the details of modified Boltzmann equations within RSII setup. But for realistic estimate one can fix  $\kappa \sim \mathcal{O}(10^{-2} - 10^{-1})$ . The baryon asymmetry is generated around a temperature  $T_B \sim 10^{10}$  GeV, which is exactly same as mass scale of the heavy Majorana neutrino and this has possibly interesting implications for the nature of dark matter. The observed value of the baryon asymmetry,  $\eta_B \sim 10^{-9}$  [49] is obtained as consequence of a large hierarchy of the heavy neutrino masses, leading to a small CP asymmetry, and the kinematical factors  $f$  and  $\kappa$ . In case of RSII setup using Eq (3.34) the lower bound on baryon asymmetry parameter can be expressed as <sup>11</sup>:

$$\eta_B \gtrsim \mathcal{O}(10^{-101}) \times \left( \frac{0.12}{r(k_*)} \right)^5 \Sigma_b^{-5}(k_L = k_0, k_*) \times \left( \frac{\sigma}{M_p^4} \right)^2. \quad (3.37)$$

which implies the following possibilities within RSII setup:

1. For the large tensor-to-scalar ratio the significant features of baryon asymmetry can be possible to detect in future. For an example we consider a situation where the tensor-to-scalar ratio is,  $r(k_*) \sim 0.12$  and in such a case the lower bound of baryon asymmetry is given by  $\eta_B \gtrsim 10^{-14}$  in RSII braneworld. This also implies that in this case it is highly possible to achieve the observed baryon asymmetry parameter,  $\eta_B \sim 10^{-9}$  by adjusting the regulating factor as well the brane tension of RSII setup at the pivot scale  $k_* \sim 0.002 \text{ Mpc}^{-1}$  by following the upper bound as stated in Eq (3.33). In case of low energy regime of RSII or equivalently for GR prescribed setup the lower bound of baryon asymmetry is given by  $\eta_B \gtrsim 10^{-26}$  with  $r(k_*) \sim 0.12$ .
2. For very small tensor-to-scalar ratio the baryon asymmetry is largely suppressed and can't be possible to detect via future experiments. For an example if tensor-to-scalar ratio,  $r(k_*) \sim 10^{-29}$  then the lower bound of baryon asymmetry parameter is given by  $\eta_B \gtrsim 10^{-30}$  in RSII braneworld. Similarly in the low energy regime of RSII or in GR limit the lower bound of baryon asymmetry is given by  $\eta_B \gtrsim 10^{-33}$  with  $r(k_*) \sim 0.12$ .

---

<sup>11</sup>In case of GR prescribes setup the lower bound of the CP asymmetry parameter can be written as:

$$\eta_B \gtrsim \mathcal{O}(10^{-119}) \times \left( \frac{0.12}{r(k_*)} \right)^3 \Sigma^{-3}(k_L = k_0, k_*). \quad (3.36)$$

## 4 BraneInflamagnetogenesis via reheating

### 4.1 Basic assumptions

Before going to the critical details of the computation, let me first briefly mention the underlying assumptions and basics of the present setup:

- The primordial magnetic field is created via quantum vacuum fluctuation and amplified during the epoch of inflation.
- Conformal invariance is restored at the end of inflation such that the magnetic field subsequently decays as  $a^{-2}$ , where  $a$  is the cosmological scale factor. Consequently the physical strength of the magnetic field today on the large scale is given by:

$$B_0 = \frac{B_{end}}{(1 + z_{end})^2}. \quad (4.1)$$

where  $B_0$  and  $B_{end}$  are the magnetic field today and at the end of inflation respectively. Also  $z_{end}$  signifies the redshift at the end of inflation and in terms of scale factor it is defined as:

$$z_{end} = \frac{a_0}{a_{end}} - 1. \quad (4.2)$$

In this work we will explicitly show that for all classes of the models of brane inflationary magnetogenesis the redshift  $z_{end}$  depends on the properties of reheating. During the epoch of inflation the corresponding wave number can be expressed as:

$$\frac{k_*}{a} = \frac{k_*}{a_0} (1 + z_{end}) e^{\mathcal{N}_{end;b} - \mathcal{N}_b} \quad (4.3)$$

where the subscript “b” is used to specify the braneworld gravity setup and exactly consistent with Eq (4.2).

- Further I assume the instantaneous transitions between inflation, reheating, radiation and matter dominated epoch one can write:

$$(1 + z_{end}) = (1 + z_{eq}) \left( \frac{\rho_{reh}}{\rho_{eq}} \right)^{1/4} \left( \frac{a_{reh}}{a_{end}} \right) \quad (4.4)$$

where the subscript “reh” and “eq” stand for end of reheating and the matter radiation equality.

- I also assume that at the present epoch the contribution from the correction coming from the non-relativistic neutrinos are negligibly small and so that I neglected the contribution from the computation.

## 4.2 Reheating parameter

Let us first start with the reheating parameter  $R_{reh}$  defined by <sup>12</sup> [59]:

$$R_{rad} \equiv \frac{a_{end}}{a_{reh}} \left( \frac{\rho_{end}}{\rho_{reh}} \right)^{1/4}, \quad (4.5)$$

where the subscript “reh” can be interpreted as the end of reheating era and also the beginning of radiation dominated era. More precisely  $R_{reh}$  measures the deviation between reheating and radiation dominated era. Now using Eq (4.5) in Eq (4.4) one can write:

$$(1 + z_{end}) = (1 + z_{eq}) \times \left( \frac{a_{eq}}{a_{reh}} \right) \times \left( \frac{a_{reh}}{a_{end}} \right) = \frac{1}{R_{rad}} \left( \frac{\rho_{end}}{\mathcal{A}_{reh}\rho_\gamma} \right)^{1/4} \quad (4.6)$$

where in the high energy regime of RSII braneworld the radiation energy density can be expressed as:

$$\rho_\gamma = \sqrt{6\sigma\Omega_{rad}}H_0M_p \quad (4.7)$$

represents the energy density of radiation at present epoch and

$$\mathcal{A}_{reh} \equiv \frac{g_{reh}}{g_0} \left( \frac{q_0}{q_{reh}} \right)^{4/3} \quad (4.8)$$

is the measure of the change of relativistic degrees of freedom between the reheating epoch and present epoch. Also  $q$  and  $g$  denotes the number of entropy and relativistic degrees of freedom at the epoch of interest respectively. Here  $H_0$  represents the Hubble parameter at the present epoch and  $\Omega_{rad}$  signifies the dimensionless density parameter during radiation dominated era. To proceed further here I start with the expression for the number of e-foldings at any arbitrary momentum scale] as [60–64]:

$$\mathcal{N}_b(k) = 71.21 - \ln \left( \frac{k}{k_0} \right) + \frac{1}{4} \ln \frac{V_*}{M_p^4} + \frac{1}{4} \ln \frac{V_*}{\rho_{end}} + \frac{1 - 3\bar{w}_{reh}}{12(1 + \bar{w}_{reh})} \ln \left( \frac{\rho_{reh}}{\rho_{end}} \right) \quad (4.9)$$

where  $\rho_{end}$  is the energy density at the end of inflation,  $\rho_{reh}$  is an energy scale during reheating,  $k_0 = a_0H_0$  is the present Hubble scale,  $V_*$  corresponds to the potential energy when the relevant modes left the Hubble patch during inflation corresponding to the momentum scale  $k_* \approx k_{cmb}$ , and  $\bar{w}_{reh}$  characterizes the effective equation of state parameter between the end of inflation and the energy scale during reheating. Further using Eq (4.9) one can write:

$$\Delta\bar{\mathcal{N}}_b = \mathcal{N}_{reh;b} - \mathcal{N}_{end;b} = \ln \left( \frac{a_{reh}}{a_{end}} \right) = \ln \left( \frac{k_{end}}{k_{reh}} \right). \quad (4.10)$$

---

<sup>12</sup>If I fix  $R_{rad} = 1$  then from Eq (4.5) it implies that  $\rho \propto a^{-4}$ , which exactly mimics the role of the energy density during radiation dominated era.



Now using only the energy conservation one can derive the following expression for the reheating energy density:

$$\rho_{reh} = \rho_{end} \exp \left[ -3 \int_{\mathcal{N}_{end;b}}^{\mathcal{N}_{reh;b}} (1 + w(\mathcal{N}_b)) d\mathcal{N}_b \right] \approx \rho_{end} \exp [-3\Delta\bar{\mathcal{N}}_b (1 + \bar{w}_{reh})] \quad (4.11)$$

where  $\Delta\bar{\mathcal{N}}_b$  is defined in Eq (4.10) and the mean equation of state parameter  $\bar{w}_{reh}$  is defined as:

$$\bar{w}_{reh} \equiv \frac{\int_{\mathcal{N}_{end;b}}^{\mathcal{N}_{reh;b}} w(\mathcal{N}_b) d\mathcal{N}_b}{\Delta\bar{\mathcal{N}}_b}. \quad (4.12)$$

where  $w(\mathcal{N}_b) = P(\mathcal{N}_b)/\rho(\mathcal{N}_b)$  represents the instantaneous equation of state parameter. Further using Eq (4.11) in Eq (4.5) one can derive the following expression for reheating parameter:

$$R_{rad} = \left( \frac{\rho_{reh}}{\rho_{end}} \right)^{\frac{1-3\bar{w}_{reh}}{12(1+\bar{w}_{reh})}}. \quad (4.13)$$

Here Eq (4.13) also implies that for  $\bar{w}_{reh} = 1/3$  the reheating parameter  $R_{rad} = 1$ .

### 4.3 Evading magnetic back-reaction

To evade magnetic back-reaction on the cosmological background in this paper I consider the following two physical situations:

1. **In the first situation** the reheating epoch characterizes by the lower bound on the equation of state parameter at,  $\bar{w}_{reh} \geq 1/3$  and the corresponding energy density during reheating decays very faster compared to the energy density during radiation dominated era. In this case, the magnetic back-reaction on the length scales of interest is evaded for the following constraint on the ratio of the energy densities [59]:

$$\frac{\rho_{\mathbf{B}}(z_{reh})}{\rho_{reh}} = \frac{\rho_{\mathbf{B}_0}}{\rho_{\gamma}} < 1 \quad (4.14)$$

Now further using the Planckian unit system one can write,  $1 \text{ Gauss} \simeq 3.3 \times 10^{-57} M_p^2$  and using this unit conversion the photon energy density can be written in terms of the magnetic unit as,  $\rho_{\gamma} \simeq 5.7 \times 10^{-125} M_p^4 = 5.2 \times 10^{-12} \text{ Gauss}^2$  [59]. Using Eq (4.13) one can further show that for  $\bar{w}_{reh} \geq 1/3$  the reheating parameter  $R_{rad} \geq 1$ . This clearly implies that magnetic back-reaction effect can be evaded using this constraint.

2. **In the second situation** the reheating epoch characterizes by  $\bar{w}_{reh} < 1/3$  and the corresponding energy density of the magnetic field dominates over the energy density during reheating epoch. Within this prescription the effect of magnetic

back-reaction can be neglected, provided the magnetic energy density remains smaller compared to the background total energy density at any epoch i.e.

$$\frac{\rho_{B_{end}}}{\rho_{end}} < 1. \quad (4.15)$$

where the magnetic energy density  $\rho_{B_{end}}$  can be written in terms of the energy density at the end of inflationary epoch as:

$$\rho_{B_{end}} = \frac{B_0^2}{2R_{rad}^4 \rho_\gamma} \rho_{end}. \quad (4.16)$$

Further substituting Eq (4.16) in Eq (4.15) one can compute the lower bound on the reheating parameter as [59]:

$$R_{rad} > \frac{\sqrt{B_0}}{(2\rho_\gamma)^{1/4}}. \quad (4.17)$$

The physical interpretation of the bound on reheating parameter is as follows:

- **Firstly** it is important to note that the lower bound on reheating parameter is true for any models of inflation and completely independent on any prior knowledge of inflationary models.
- **Secondly** to hold this bound it necessarily requires that the conformal invariance has to be satisfied during the decelerating phase of the Universe.

Further using Eq (4.11), eq (4.13) and Eq (4.17) I get the following simplified expression for the reheating constraint:

$$\frac{\sqrt{B_0}}{(2\rho_\gamma)^{1/4}} \exp \left[ \frac{\Delta\bar{\mathcal{N}}_b}{4} (1 - 3\bar{w}_{reh}) \right] < 1 \quad (4.18)$$

from which one can compute the following analytical constraint on the mean equation of state parameter  $\bar{w}_{reh}$  as:

$$\bar{w}_{reh} < \frac{1}{3} \left( 1 + \frac{4}{\Delta\bar{\mathcal{N}}_b} \ln \left( \frac{\sqrt{B_0}}{(2\rho_\gamma)^{1/4}} \right) \right) \quad (4.19)$$

For an example if I fix the magnetic field at the present epoch within  $B_0 \sim \mathcal{O}(10^{-15} \text{ Gauss} - 10^{-9} \text{ Gauss})$  then the lower bound of the reheating parameter is constrained within  $R_{rad} > \mathcal{O}(1.76 \times 10^{-5} - 10^{-2})$ . Consequently the bound on the mean equation of state parameter  $\bar{w}_{reh}$  can be computed as:

$$\bar{w}_{reh} < \frac{1}{3} \left( 1 + \frac{\mathcal{C}}{\Delta\bar{\mathcal{N}}_b} \right) \quad (4.20)$$

where the numerical factor  $\mathcal{C} \sim \mathcal{O}(18.42 - 43.81) > 0$  for  $B_0 \sim \mathcal{O}(10^{-15} \text{ Gauss} - 10^{-9} \text{ Gauss})$ .

## 5 Reheating constraints on braneinflation magnetogenesis

To derive the expression for the scale of reheating and also its connection with the inflationary magnetogenesis within RSII we start with Eq (4.13) and using this input one can write:

$$\rho_{reh} = \rho_{end} R_{rad}^{\frac{12(1+\bar{w}_{reh})}{1-3\bar{w}_{reh}}}. \quad (5.1)$$

Further using the lower limit of the reheating parameter as stated in Eq (4.17), one can derive the lower bound of the reheating energy density as:

$$\rho_{reh} > \rho_{end} \left( \frac{B_0}{\sqrt{2\rho_\gamma}} \right)^{\frac{6(1+\bar{w}_{reh})}{1-3\bar{w}_{reh}}} = \rho_{end} \left( \frac{B_0}{\sqrt{2\rho_\gamma}} \right)^{-2 \left( 1 + \frac{\Delta \tilde{\mathcal{N}}_b}{\ln \left( \frac{\sqrt{B_0}}{(2\rho_\gamma)^{1/4}} \right)} \right)}. \quad (5.2)$$

Now in the high density or high energy regime of RSII,  $\rho \gg \sigma$  and using the Friedmann equation one can write [39, 40]:

$$H \approx \frac{\rho}{\sqrt{6\sigma} M_p}. \quad (5.3)$$

where  $\sigma$  is the brane tension in RSII setup. Hence using Eq (5.3) the lower bound of the reheating energy density can be recast within RSII setup as <sup>13</sup>:

$$\rho_{reh} > \sqrt{6\sigma} M_p H_{end} \left( \frac{B_0}{\sqrt{2\rho_\gamma}} \right)^{\frac{6(1+\bar{w}_{reh})}{1-3\bar{w}_{reh}}} = \sqrt{6\sigma} M_p H_{end} \left( \frac{B_0}{\sqrt{2\rho_\gamma}} \right)^{-2 \left( 1 + \frac{\Delta \tilde{\mathcal{N}}_b}{\ln \left( \frac{\sqrt{B_0}}{(2\rho_\gamma)^{1/4}} \right)} \right)} \quad (5.5)$$

where  $H_{end}$  represents the Hubble parameter at the end of reheating and additionally Eq (4.20) has to be satisfied to avoid magnetic back-reaction. Here Eq (5.5) implies that if the magnetic field is generated via inflation in braneworld then by knowing the Hubble scale at the end of inflation as well as the constraint on the brane tension  $\sigma$  it is possible to constraint the lower bound of the scale of reheating. It is important to note that if  $\bar{w}_{reh} \rightarrow 1/3$  the equality in Eq (5.5) will not hold at all and also in such a situation the exponent diverges i.e.  $\frac{6(1+\bar{w}_{reh})}{1-3\bar{w}_{reh}} \rightarrow \infty$ . This clearly implies that the lower bound of the reheating energy density is zero and compatible with the understandings of the physics of inflationary magnetogenesis. In the present context the field value at the end of inflation is determined by the violation of the slow-roll conditions. See Appendix

---

<sup>13</sup>In the low density regime of RSII braneworld or equivalently in GR limit the lower bound on the reheating energy density can be expressed as:

$$\rho_{reh} > \sqrt{3} M_p H_{end} \left( \frac{B_0}{\sqrt{2\rho_\gamma}} \right)^{\frac{6(1+\bar{w}_{reh})}{1-3\bar{w}_{reh}}} = \sqrt{3} M_p H_{end} \left( \frac{B_0}{\sqrt{2\rho_\gamma}} \right)^{-2 \left( 1 + \frac{\Delta \tilde{\mathcal{N}}_b}{\ln \left( \frac{\sqrt{B_0}}{(2\rho_\gamma)^{1/4}} \right)} \right)} \quad (5.4)$$

8.1 for the details. Consequently one can derive the following sets of constraints on the generic form of inflationary potential and its derivatives at the end of inflation as:

$$V(\phi_{end}) = (2M_p^2\sigma)^{1/3} \left( V'(\phi_{end}) \right)^{2/3}, \quad (5.6)$$

$$V(\phi_{end}) = (2M_p^2\sigma)^{1/2} \left( V''(\phi_{end}) \right)^{1/2}, \quad (5.7)$$

$$V(\phi_{end}) = (4M_p^4\sigma^2)^{1/4} \left( V'(\phi_{end})V'''(\phi_{end}) \right)^{1/2}, \quad (5.8)$$

$$V(\phi_{end}) = (8M_p^6\sigma^3)^{1/6} \left( V'(\phi_{end}) \right)^{1/3} \left( V''''(\phi_{end}) \right)^{1/6}. \quad (5.9)$$

For more stringent constraint the system need to satisfy all of the equations as mentioned in Eq (5.6-5.9) to fix the scale of inflationary potential at the end of inflation. In this case the derivatives or more precisely the Taylor expansion co-efficients of the inflationary potential at the end of inflation are not independent at all. But if the system relaxes any three of the previously mentioned constraints, then also it possible to constrain the scale of potential at the end epoch of inflation. Consequently Eq (5.5) can be recast in terms of the generic form of the inflationary potential as:

$$\rho_{reh} > V(\phi_{end}) \left( \frac{B_0}{\sqrt{2\rho_\gamma}} \right)^{\frac{6(1+\bar{w}_{reh})}{1-3\bar{w}_{reh}}} \approx V(\phi_{end}) \left( \frac{B_0}{\sqrt{2\rho_\gamma}} \right)^{-2} \left( 1 + \frac{\Delta\mathcal{N}_b}{\ln\left(\frac{\sqrt{B_0}}{(2\rho_\gamma)^{1/4}}\right)} \right) \quad (5.10)$$

Here it is important to note that during reheating both kinetic and potential contribution play crucial role in the energy density. Later I will explicitly show the estimation algorithm of  $V(\phi_{end})$  from a generic as well as for specified form of inflationary potential for the determination of the lower bound of the energy density during reheating.

In the high energy regime of RSII setup during reheating one can write the total decay width for the decay of heavy Majorana neutrinos as [29, 30]:

$$\Gamma_{total} = \Gamma_L(N_R \rightarrow L_i\Phi) + \Gamma_{L^c}(N_R \rightarrow L_i^c\Phi^c) = 3H(T_{reh}) \approx \sqrt{\frac{3}{2\sigma}} \frac{\rho_{reh}}{M_p} \quad (5.11)$$

where  $H(T_{reh})$  be the Hubble parameter during reheating and  $\rho_{reh}$  represents the energy density during reheating. In the context of statistical thermodynamics one can express the reheating energy density as:

$$\rho_{reh} = \frac{\pi^2}{30} g_* T_{reh}^4 \quad (5.12)$$

where  $g_*$  signifies the effective number of relativistic degrees of freedom. In a more generalized prescription  $g_*$  can be expressed as:

$$g_* = g_{B*} + \frac{7}{8} g_{F*} \quad (5.13)$$

where  $g_{B*}$  and  $g_{F*}$  are the number of bosonic and fermionic degrees of freedom respectively. It is worth mentioning that the reheating temperature within RSII does not depend on the initial value of the inflaton field from where inflation starts and is solely determined by the elementary particle theory of the early universe. Further using Eq (5.11) and Eq (5.12) the reheating temperature within the high energy regime of RSII setup can be expressed as <sup>14</sup> [29, 30]:

$$T_{reh} = \left( \frac{30}{\pi^2 g_*} \right)^{1/4} \times (\Gamma_{total} M_p)^{1/4} \times \left( \frac{2\sigma}{3} \right)^{1/8}. \quad (5.15)$$

On the other hand the reheating temperature can be expressed in terms of the tensor-to-scalar ratio as:

$$T_{reh} \approx \left( \frac{30}{\pi^2 g_*} \right)^{1/4} \times (1.96 \times 10^{16} \text{GeV}) \times \left( \frac{r(k_*)}{0.12} \right)^{1/4}. \quad (5.16)$$

Now eliminating reheating temperature from Eq (5.15) and Eq (5.16) one can express the total decay width in terms of inflationary tensor-to-scalar ratio as <sup>15</sup>:

$$\Gamma_{total} = 4.23 \times 10^{-9} M_p^3 \times \sqrt{\frac{3}{2\sigma}} \times \left( \frac{r(k_*)}{0.12} \right). \quad (5.18)$$

Further combining Eq (4.11) and Eq (5.12) the energy density of inflaton at the end of inflation can be expressed in terms of tensor-to-scalar ratio as:

$$\rho_{end} \approx V(\phi_{end}) = (1.96 \times 10^{16} \text{GeV})^4 \times \left( \frac{r(k_*)}{0.12} \right) \times \exp [3(1 + \bar{w}_{reh}) \Delta \bar{\mathcal{N}}_b]. \quad (5.19)$$

Similarly using Eq (5.19) in Eq (5.10) the reheating energy density or more precisely the scale of reheating can be expressed in terms of the tensor-to-scalar ratio, mean equation of reheating  $\bar{w}_{reh}$  and magnetic field at the present epoch as:

$$\rho_{reh} > (1.96 \times 10^{16} \text{GeV})^4 \times \left( \frac{r(k_*)}{0.12} \right) \times \exp [3(1 + \bar{w}_{reh}) \Delta \bar{\mathcal{N}}_b] \times \left( \frac{B_0}{\sqrt{2\rho_\gamma}} \right)^{\frac{6(1+\bar{w}_{reh})}{1-3\bar{w}_{reh}}}. \quad (5.20)$$

---

<sup>14</sup>In the low energy regime of RSII or equivalently in the GR limit the reheating temperature can be expressed as [63, 65, 66]:

$$T_{reh} = \left( \frac{30}{\pi^2 g_*} \right)^{1/4} \times \left( \frac{\Gamma_{total} M_p}{\sqrt{3}} \right)^{1/2}. \quad (5.14)$$

<sup>15</sup>In the low energy regime of RSII or equivalently in the GR limit total decay width of the heavy Majorana neutrino can be written as:

$$\Gamma_{total} = 1.13 \times 10^{-4} M_p \times \left( \frac{r(k_*)}{0.12} \right)^{1/2}. \quad (5.17)$$

Further applying the constraint in the mean equation of reheating parameter as stated in Eq (4.19) the lower bound of the scale of reheating energy density can be recast as:

$$\rho_{reh} > (1.96 \times 10^{16} \text{GeV})^4 \times \left( \frac{r(k_*)}{0.12} \right) \times \exp [4\Delta\bar{\mathcal{N}}_b] \times \left( \frac{B_0}{\sqrt{2\rho_\gamma}} \right)^{-\frac{4\Delta\bar{\mathcal{N}}_b}{\ln\left(\frac{B_0}{\sqrt{2\rho_\gamma}}\right)}}. \quad (5.21)$$

Next I will explicitly derive the expression for the density parameter during radiation dominated epoch ( $\Omega_{rad}$ ) and further I will connect this to the density parameter of the magnetic field ( $\Omega_{B_{end}}$ ). To serve this purpose we start with the analysis in the high energy regime of the RSII braneworld in which the dimensionless density parameter can be expressed as:

$$\Omega = \frac{\rho^2}{\rho_c \rho_0} \quad (5.22)$$

where the critical energy density in RSII braneworld can be written as:

$$\rho_c = 2\sigma \quad (5.23)$$

and the energy density at the present epoch can be written as:

$$\rho_0 = 3M_p^2 H_0^2. \quad (5.24)$$

Now using Eq (4.6) in Eq (4.16) one can write the magnetic energy density in terms of redshift as:

$$\rho_{B_{end}} = \frac{B_0^2}{2} (1 + z_{eq})^4 \exp [\Delta\bar{\mathcal{N}}_b (1 - 3\bar{w}_{reh})] \quad (5.25)$$

and using Eq (5.25) the dimensionless density parameter for magnetic field can be written as:

$$\Omega_{B_{end}} = \frac{B_0^4}{24\sigma H_0^2 M_p^2} (1 + z_{eq})^8 \exp [2\Delta\bar{\mathcal{N}}_b (1 - 3\bar{w}_{reh})]. \quad (5.26)$$

In the high energy regime of RSII braneworld one can write the density parameter at the end of inflation in terms of the density parameter at the radiation dominated era and redshift as:

$$\Omega_{end} = (1 + z_{eq})^8 \Omega_{rad}. \quad (5.27)$$

Further substituting Eq (5.29) in Eq (5.28) I get the following constraint relationship:

$$\Omega_{B_{end}} = \frac{B_0^4 \Omega_{end}}{24\sigma H_0^2 M_p^2 \Omega_{rad}} \exp [2\Delta\bar{\mathcal{N}}_b (1 - 3\bar{w}_{reh})]. \quad (5.28)$$

Next using Eq (5.19) one can write down the expression for the dimensionless parameter at the end of inflationary epoch as:

$$\Omega_{end} = \frac{M_p^6}{6\sigma H_0^2} \times (1.79 \times 10^{-17}) \times \left( \frac{r(k_*)}{0.12} \right)^2 \times \exp [6(1 + \bar{w}_{reh}) \Delta\bar{\mathcal{N}}_b]. \quad (5.29)$$

Further applying the constraint in the mean equation of reheating parameter as stated in Eq (4.19) the dimensionless density parameter can be expressed in terms of the magnetic field at the present epoch as:

$$\Omega_{end} = \frac{M_p^6}{6\sigma H_0^2} \times (1.79 \times 10^{-17}) \times \left( \frac{r(k_*)}{0.12} \right)^2 \times \exp \left[ 8 \left( \Delta \bar{\mathcal{N}}_b + \ln \left( \frac{\sqrt{B_0}}{(2\rho_\gamma)^{1/4}} \right) \right) \right]. \quad (5.30)$$

Finally substituting Eq (5.30) in Eq (5.28) we get <sup>16</sup>:

$$\Omega_{B_{end}} = \frac{B_0^4 M_p^4}{144\sigma^2 H_0^4 \Omega_{rad}} \times (1.79 \times 10^{-17}) \times \left( \frac{r(k_*)}{0.12} \right)^2 \times \exp [8\Delta \bar{\mathcal{N}}_b]. \quad (5.32)$$

Here the dimensionless density parameter during the epoch of radiation domination is given by the following expression:

$$\Omega_{rad} = \frac{\rho_\gamma^2}{\rho_c \rho_0} = \frac{\rho_\gamma^2}{6\sigma H_0^2 M_p^2} \quad (5.33)$$

where  $\rho_\gamma \simeq 5.7 \times 10^{-125} M_p^4 = 5.2 \times 10^{-12} \text{ Gauss}^2$ . Further using Eq (5.33) in Eq (5.32) we get:

$$\Omega_{B_{end}} = \frac{B_0^4 M_p^6}{24\sigma H_0^2 \rho_\gamma^2} \times (1.79 \times 10^{-17}) \times \left( \frac{r(k_*)}{0.12} \right)^2 \times \exp [8\Delta \bar{\mathcal{N}}_b]. \quad (5.34)$$

Next using Eq (3.9) in Eq (5.34) finally we get the following relationship between the density parameter of the magnetic field and the CP asymmetry parameter within the high energy regime of RSII braneworld as <sup>17</sup>:

$$\Omega_{B_{end}} = \frac{M_p^6}{24\sigma H_0^2 \epsilon_{\text{CP}}^2} \times (6.63 \times 10^{-83}) \times \left( \frac{r(k_*)}{0.12} \right)^2 \times \exp [8\Delta \bar{\mathcal{N}}_b]. \quad (5.36)$$

## 6 Constraining models of braneflamagnetogenesis from CMB

Before going to the details of the constraints on the various models of brane inflationary magnetogenesis from CMB, let me introduce a rescaled reheating parameter  $R_{sc}$  defined as [59]:

$$R_{sc} \equiv R_{rad} \times \frac{\rho_{end}^{1/4}}{M_p} = \left( \frac{\rho_{reh}}{\rho_{end}} \right)^{\frac{1-3\bar{w}_{reh}}{12(1+\bar{w}_{reh})}} \times \frac{\rho_{end}^{1/4}}{M_p} = \frac{a_{end}}{a_{reh}} \times \left( \frac{\rho_{end}^{1/2}}{\rho_{reh}^{1/4} M_p} \right) \quad (6.1)$$

<sup>16</sup>In the low energy regime of RSII dimensionless density parameter for magnetic field can be expressed as:

$$\Omega_{B_{end}} = \frac{B_0^2}{6M_p^2 H_0^2 \Omega_{rad}} \times (2.17 \times 10^{-5}) \times \left( \frac{r(k_*)}{0.12} \right) \times \exp [4\Delta \bar{\mathcal{N}}_b]. \quad (5.31)$$

<sup>17</sup>In the low energy regime of RSII or equivalently in Gr limit the dimensionless density parameter for magnetic field can be expressed as:

$$\Omega_{B_{end}} = \frac{1}{2\epsilon_{\text{CP}}} \times (4.17 \times 10^{-38}) \times \left( \frac{r(k_*)}{0.12} \right) \times \exp [4\Delta \bar{\mathcal{N}}_b]. \quad (5.35)$$

which is relevant for further analysis. Further using Eq (5.19) the lower bound of the rescaled reheating parameter can be expressed in terms of the tensor-to-scalar ratio and the magnetic field at the present epoch as:

$$R_{sc} > 8.07 \times 10^{-3} \times \left( \frac{r(k_*)}{0.12} \right)^{1/4} \times \exp [\Delta \bar{\mathcal{N}}_b] \times \left( \frac{B_0}{\sqrt{2\rho_\gamma}} \right). \quad (6.2)$$

In the following subsections I will explicitly discuss about the CMB constraints on two types of models of brane inflationary magnetogenesis. But in principle one can carry forward the prescribed methodology for rest of the brane inflationary models also.

### 6.1 Monomial Models

In case of monomial models the inflationary potential can be represented by the following functional form:

$$V(\phi) = V_0 \left( \frac{\phi}{M_p} \right)^\beta \quad (6.3)$$

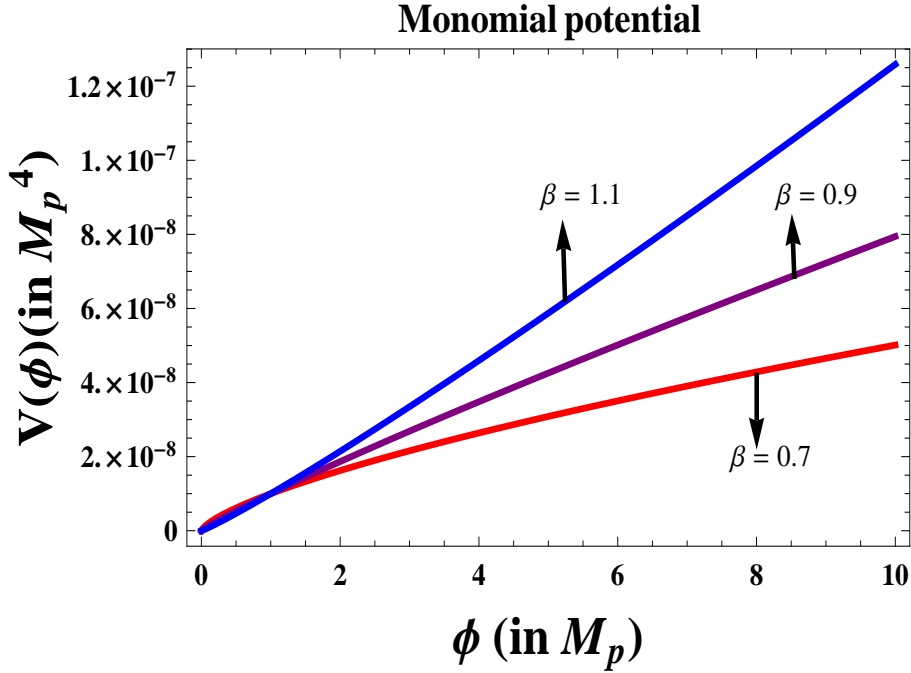


**Figure 2.** Variation of the monomial potential for the index  $\beta = 0.7, 0.9, 1.1$ . Here I fix the tunable scale at  $\sqrt[4]{V_0} = 4.12 \times 10^{-3} M_p = 10^{16} \text{ GeV}$ .

where  $V_0 = M^4$  is the tunable energy scale, which is necessarily required to fix the amplitude of the CMB anisotropies and  $\beta$  is the monomial index which characterizes the feature of the potential. The variation of the monomial potential for the index  $\beta = 0.7, 0.9, 1.1$  and the tunable scale  $\sqrt[4]{V_0} = 4.12 \times 10^{-3} M_p = 10^{16} \text{ GeV}$  is shown in fig. 2. In the present context both the rescaled reheating parameter  $R_{sc}$  and the energy



density at the end of inflation  $\rho_{end}$  are constrained<sup>18</sup>. To analyze the features of the potential in detail here I start with the definition of number of e-foldings  $\Delta\mathcal{N}_b(\phi)$  in the high energy regime of RSII setup (see Appendix 8.1 for details), using which I get:

$$\Delta\mathcal{N}_b(\phi) = \frac{V_0}{2\sigma\beta(\beta+2)M_p^{\beta+2}} \left( \phi^{\beta+2} - \phi_{end}^{\beta+2} \right). \quad (6.6)$$

Further setting  $\phi = \phi_{cmb}$  in Eq (6.6), the field value at the horizon crossing can be computed as:

$$\phi_{cmb} = \phi_{end} \left[ 1 + \frac{2\sigma\beta(\beta+2)M_p^{\beta+2}\Delta\mathcal{N}_b}{\phi_{end}^{\beta+2}V_0} \right]^{\frac{1}{\beta+2}} \quad (6.7)$$

where  $\phi_{end}$  represents the field value of inflaton at the end of inflation. Within RSII setup from the violation of the slow-roll conditions one can compute:

$$\phi_{end} \approx \left( \frac{2\sigma\beta^2}{V_0} \right)^{\frac{1}{\beta+2}} M_p. \quad (6.8)$$

From monomial models of inflation the scale of the potential at the horizon crossing and at the end of inflation can be computed as:

$$\rho_{cmb} \approx V(\phi_{cmb}) = V_0 \left( \frac{\phi_{cmb}}{M_p} \right)^\beta = V_0^{\frac{2}{\beta+2}} (2\sigma\beta^2)^{\frac{\beta}{\beta+2}} \left[ 1 + \left( 1 + \frac{2}{\beta} \right) \Delta\mathcal{N}_b \right]^{\frac{\beta}{\beta+2}}, \quad (6.9)$$

$$\rho_{end} \approx V(\phi_{end}) = V_0 \left( \frac{\phi_{end}}{M_p} \right)^\beta = V_0^{\frac{2}{\beta+2}} (2\sigma\beta^2)^{\frac{\beta}{\beta+2}}. \quad (6.10)$$

Further using the consistency condition in the high energy regime of RSII braneworld, as stated in Eq (8.2) of the Appendix C, one can derive the following expressions for the amplitude of the scalar power spectrum, tensor to scalar ratio and scalar spectral tilt as:

$$P_S(k_*) = \frac{V_0^{\frac{2}{\beta+2}} (2\sigma\beta^2)^{\frac{\beta}{\beta+2}}}{36\pi^2} \left[ 1 + \left( 1 + \frac{2}{\beta} \right) \Delta\mathcal{N}_b \right]^{\frac{2(\beta+1)}{\beta+2}}, \quad (6.11)$$

$$r(k_*) = \frac{24}{\left[ 1 + \left( 1 + \frac{2}{\beta} \right) \Delta\mathcal{N}_b \right]}, \quad (6.12)$$

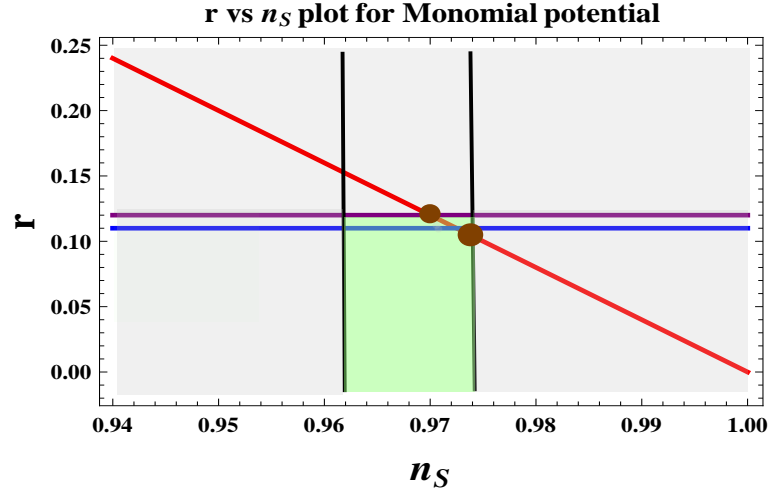
$$n_S(k_*) - 1 \approx -\frac{6}{\left[ 1 + \left( 1 + \frac{2}{\beta} \right) \Delta\mathcal{N}_b \right]}. \quad (6.13)$$

---

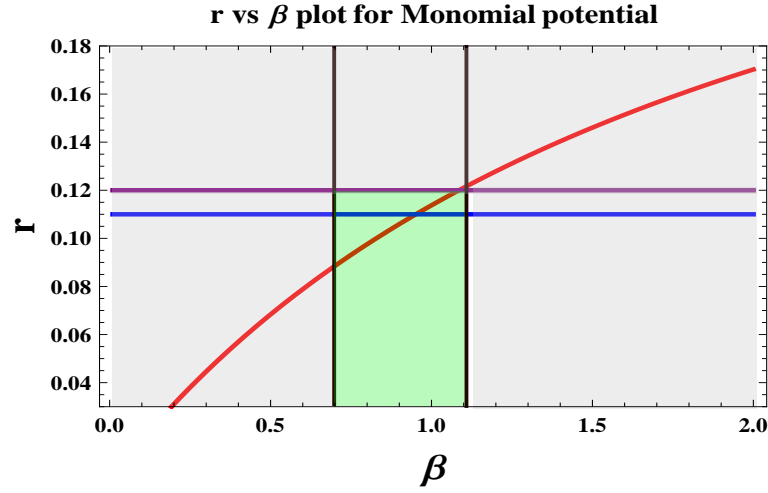
<sup>18</sup>After marginalization over the monomial index of the potential within  $0.2 < \beta < 5$  and over the cosmological parameters the following CMB constraints are obtained within  $2\sigma$  CL [73]:

$$R_{sc} > 2.81 \times 10^{-13}, \quad (6.4)$$

$$4 \times 10^{15} \text{ GeV} < \rho_{end}^{1/4} < 1.2 \times 10^{16} \text{ GeV}. \quad (6.5)$$



(a)  $r$  vs  $n_S$ .



(b)  $r$  vs  $\beta$ .

**Figure 3.** Behaviour of the tensor-to-scalar ratio  $r$  with respect to **3(a)** the scalar spectral index  $n_S$  and **3(b)** the characteristic parameter of the monomial potential  $\beta$ . The purple and blue coloured line represent the upper bound of tensor-to-scalar ratio allowed by Planck+BICEP2+Keck Array joint constraint and only Planck 2015 data respectively. The small and the big bubbles represent two consecutive points in  $r - n_S$  plane, where for the small bubble  $\Delta\mathcal{N}_b = 50, r = 0.124, n_S = 0.969$  and for the big bubble  $\Delta\mathcal{N}_b = 70, r = 0.121, n_S = 0.970$  respectively. The green shaded region bounded by two vertical black coloured lines represent the Planck  $2\sigma$  allowed region and the rest of the light grey shaded region is disfavoured by the Planck data and Planck+ BICEP2+Keck Array joint constraint. From **3(a)** it is observed that, within  $50 < \Delta\mathcal{N}_b < 70$  the monomial potential is favoured only for the characteristic index  $0.7 < \beta < 1.1$ , by Planck 2015 data and Planck+ BICEP2+Keck Array joint analysis. In **3(b)** I have explicitly shown that the in  $r - \beta$  plane the observationally favoured window for the monomial index is  $0.7 < \beta < 1.1$ .

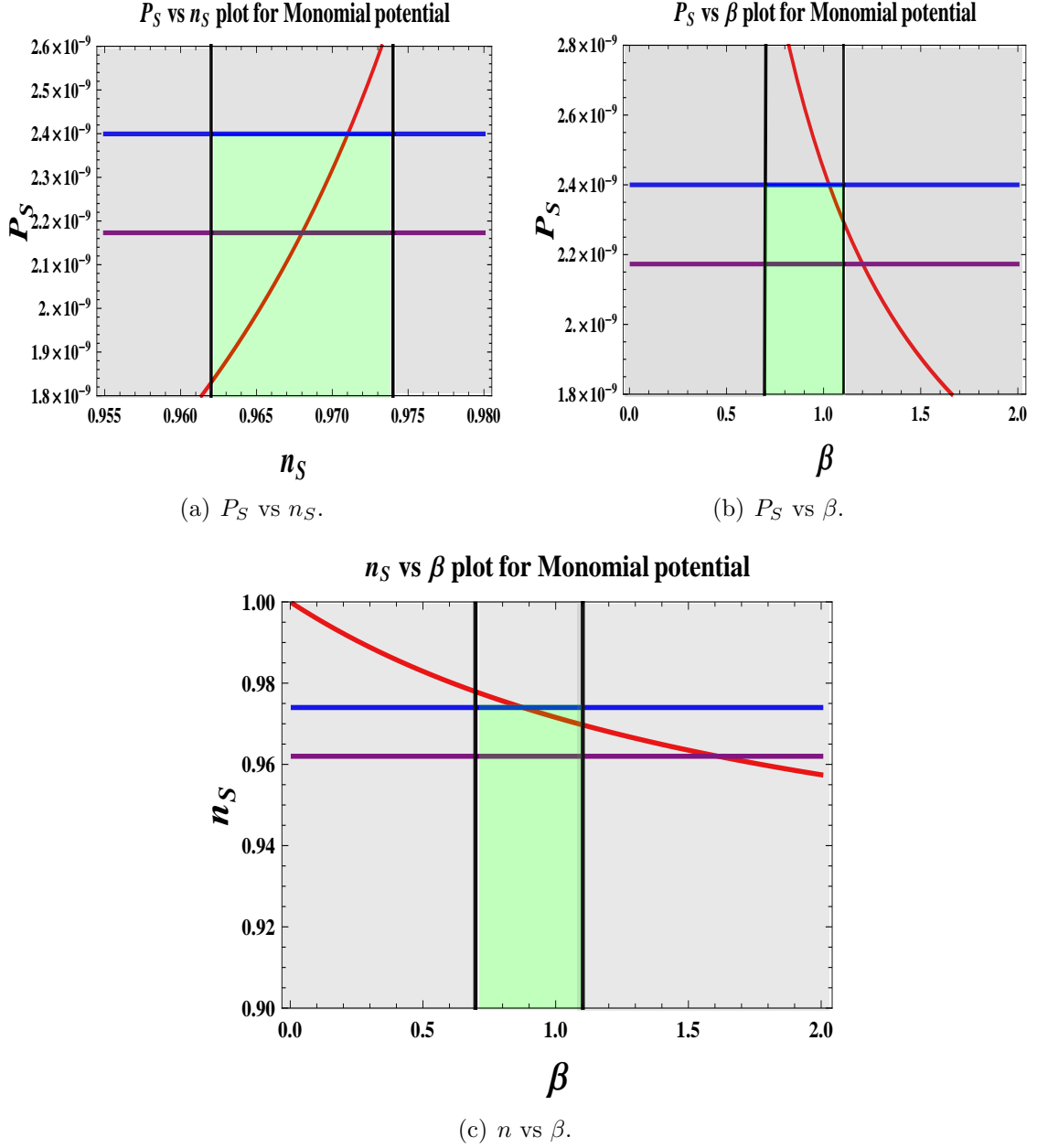


**Figure 4.** Variation of the [4\(a\)](#) scalar power spectrum  $P_S$  vs scalar spectral index  $n_S$ , [4\(b\)](#) scalar power spectrum  $P_S$  vs index  $\beta$  and [4\(c\)](#) scalar power spectrum  $n_S$  vs index  $\beta$ . The purple and blue coloured line represent the upper and lower bound allowed by WMAP+Planck 2015 data respectively. The green dotted region bounded by two vertical black coloured lines represent the Planck  $2\sigma$  allowed region and the rest of the light grey shaded region is disfavoured by the Planck+WMAP constraint.

and to satisfy the joint constraint on the scalar spectral tilt and upper bound of tensor-to-scalar ratio as observed by Planck (2013 and 2015) and Planck+BICEP2+Keck Array, one need the following constraint on the monomial index  $\beta$  of the inflationary

potential <sup>19</sup>:

$$\beta < \frac{2}{\frac{199}{\Delta\mathcal{N}_b} - 1}. \quad (6.14)$$

The behaviour of the tensor-to-scalar ratio  $r$  with respect to the scalar spectral index  $n_S$  and the characteristic parameter of the monomial potential  $\beta$  are plotted in fig. 3(a) and fig. 3(b) respectively. From 3(a) it is observed that, within  $50 < \Delta\mathcal{N}_b < 70$  the monomial potential is favoured only for the characteristic index  $0.7 < \beta < 1.1$ , by Planck 2015 data and Planck+ BICEP2+Keck Array joint analysis. In 3(b) I have explicitly shown that the in  $r - \beta$  plane the observationally favoured window for the monomial index is  $0.7 < \beta < 1.1$ . Additionally it is important to note that, for monomial potentials embedded in the high energy regime of RSII braneworld, the consistency relation between tensor-to-scalar ratio  $r$  and the scalar spectral  $n_S$  is given by,

$$r \approx 4(1 - n_S). \quad (6.15)$$

On the other hand in the low energy regime of RSII braneworld or equivalently in the GR limiting situation, the consistency relation between tensor-to-scalar ratio  $r$  and the scalar spectral  $n_S$  is modified as,

$$r \approx \frac{8}{3}(1 - n_S). \quad (6.16)$$

This also clearly suggests that the estimated numerical value of the tensor-to-scalar ratio from the GR limit is different compared to its value in the high density regime of the RSII braneworld. To justify the validity of this statement, let me discuss a very simplest situation, where the scalar spectral index is constrained within  $0.969 < n_S < 0.970$ , as appearing in this paper. Now in such a case using the consistency relation in GR limit one can easily compute that the tensor-to-scalar is constrained within the window,  $0.080 < r < 0.083$ , which is pretty consistent with Planck 2015 result.

Variation of the 4(a) scalar power spectrum  $P_S$  vs scalar spectral index  $n_S$ , 4(b) scalar power spectrum  $P_S$  vs index  $\beta$  and 4(c) scalar power spectrum  $n_S$  vs index  $\beta$ . The purple and blue coloured line represent the upper and lower bound allowed by WMAP+Planck 2015 data respectively. The green dotted region bounded by two vertical black coloured lines represent the Planck  $2\sigma$  allowed region and the rest of the light grey shaded region is disfavoured by the Planck+WMAP constraint. From the fig. 4(a)-fig. 4(c) it is clearly observed that the monomial index of the the inflationary potential is constrained within the window  $0.7 < \beta < 1.1$  for the amplitude of the scalar power spectrum,  $2.3794 \times 10^{-9} < P_S < 2.3798 \times 10^{-9}$  and scalar spectral tilt,  $0.969 < n_S < 0.970$ . Now using Eq (6.11), Eq (6.12) and Eq (6.13) one can write another consistency relation among the amplitude of the scalar power spectrum  $P_S$ , tensor-to-scalar ratio  $r$  and scalar spectral index  $n_S$  for monomial potentials embedded

---

<sup>19</sup>For a realistic estimate, if we fix  $\Delta\mathcal{N}_b \approx \mathcal{O}(50 - 70)$ , then the monomial index  $\beta$  is constrained as,  $0.7 < \beta < 1.1$ .

in the high density regime of RSII braneworld as:

$$P_S = \frac{V_0^{\frac{2}{\beta+2}} (2\sigma\beta^2)^{\frac{\beta}{\beta+2}}}{36\pi^2} \left[ \frac{6}{1-n_S} \right]^{\frac{2(\beta+1)}{\beta+2}} = \frac{V_0^{\frac{2}{\beta+2}} (2\sigma\beta^2)^{\frac{\beta}{\beta+2}}}{36\pi^2} \left[ \frac{24}{r} \right]^{\frac{2(\beta+1)}{\beta+2}}. \quad (6.17)$$

Further using Eq (3.21), I get the following stringent constraint on the tunable energy scale of the monomial models of inflation:

$$V_0 = M^4 < \frac{(2.12 \times 10^{-11} M_p^4)^{1+\frac{\beta}{2}}}{(2\sigma\beta^2)^{\frac{\beta}{2}}}. \quad (6.18)$$

The variation of the energy scale of the monomial potential with respect to the characteristic index  $\beta$  is shown in fig. 5(a) and fig. 5(b), for the fixed the value of the brane tension at  $\sigma \sim 10^{-9} M_p^4$  and  $\sigma \sim 10^{-15} M_p^4$  respectively. This analysis explicitly shows that for  $\sigma \sim 5 \times 10^{-16} M_p^4$  the tensor-to-scalar ratio and scalar spectral tilt are constrained within the window,  $0.121 < r < 0.124$  and  $0.969 < n_s < 0.970$ , which is consistent with  $2\sigma$  CL constraints.

Also using Eq (6.3) the mean equation of state parameter during reheating can be computed as <sup>20</sup>:

$$\bar{w}_{reh} = \frac{\beta - 2}{\beta + 2}. \quad (6.19)$$

Variation of the mean equation of state parameter with respect to the monomial index  $\beta$  is explicitly shown in fig. 6. The green shaded region bounded by two vertical black coloured lines and two black coloured horizontal line represent the Planck  $2\sigma$  allowed region and the rest of the light grey shaded region is disfavoured by the Planck data and Planck+ BICEP2+Keck Array joint constraint.

Hence using Eq (4.19), I get the following stringent constraint on the upper bound on the monomial index  $\beta$  of the inflationary potential in terms of the magnetic field at the present epoch as:

$$\beta < \frac{4 \left( 1 + \frac{1}{\Delta\bar{\mathcal{N}}_b} \ln \left( \frac{\sqrt{B_0}}{(2\rho_\gamma)^{1/4}} \right) \right)}{\left( 1 - \frac{2}{\Delta\bar{\mathcal{N}}_b} \ln \left( \frac{\sqrt{B_0}}{(2\rho_\gamma)^{1/4}} \right) \right)} \quad (6.20)$$

where

$$\Delta\bar{\mathcal{N}}_b = \mathcal{N}_{reh;b} - \mathcal{N}_{cmb;b} + \Delta\mathcal{N}_b. \quad (6.21)$$

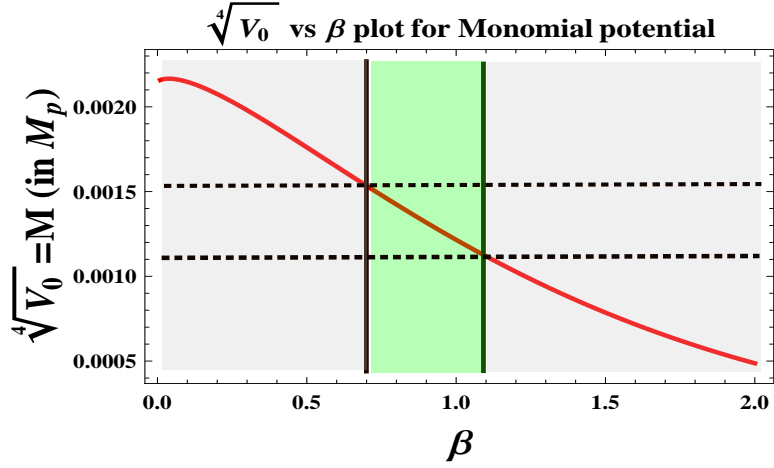
Here using Eq (6.14) in Eq one can derive the following constraint on  $\Delta\bar{\mathcal{N}}_b$  as:

$$\Delta\bar{\mathcal{N}}_b < \frac{398}{\Delta\mathcal{N}_b} \ln \left( \frac{\sqrt{B_0}}{(2\rho_\gamma)^{1/4}} \right). \quad (6.22)$$

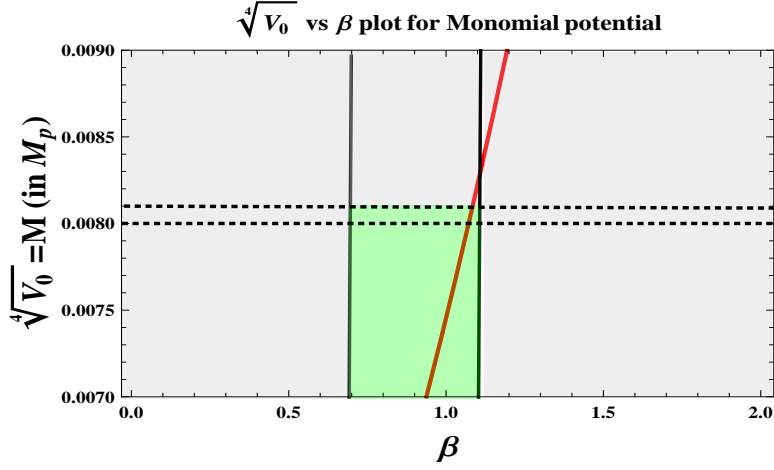
Further using Eq (5.20) the reheating energy density can be computed as:

---

<sup>20</sup>To satisfy the CMB constraints, if we fix  $\Delta\mathcal{N}_b \approx \mathcal{O}(50 - 70)$ , then the mean equation of state parameter  $\bar{w}_{reh}$  is constrained as,  $-0.48 < \bar{w}_{reh} < -0.29$ .



(a)  $V_0^{1/4}$  vs  $\beta$  for  $\sigma \sim 10^{-9} M_p^4$ .



(b)  $V_0^{1/4}$  vs  $\beta$  for  $\sigma \sim 5 \times 10^{-16} M_p^4$ .

**Figure 5.** Variation of the energy scale of the monomial potential with respect to the characteristic index  $\beta$ . The green shaded region bounded by two vertical black coloured lines and two black coloured horizontal line represent the Planck  $2\sigma$  allowed region and the rest of the light grey shaded region is disfavoured by the Planck data and Planck+ BICEP2+Keck Array joint constraint. In 5(a) and 5(b) I have fixed the value of the brane tension at  $\sigma \sim 10^{-9} M_p^4$  and  $\sigma \sim 10^{-15} M_p^4$  respectively. This analysis explicitly shows that the  $2\sigma$  allowed window for the parameter  $\beta$  within  $0.7 < \beta < 1.1$  constraints the scale of inflation within  $1.1 \times 10^{-3} M_p < \sqrt[4]{V_0} < 1.5 \times 10^{-3} M_p$  for  $\sigma \sim 10^{-9} M_p^4$  and  $8.08 \times 10^{-3} M_p < \sqrt[4]{V_0} < 8.13 \times 10^{-3} M_p$  for  $\sigma \sim 5 \times 10^{-16} M_p^4$ . For the first case the tensor-to-scalar ratio and scalar spectral tilt are constrained within the window,  $4.15 \times 10^{-5} < r < 1.44 \times 10^{-4}$  and  $n_S \sim 0.99$ . Here for  $\sigma \sim 10^{-9} M_p^4$  the value of  $r$  is consistent with the upper bound on tensor-to-scalar ratio, but the value of scalar spectral tilt is outside the  $2\sigma$  CL. On the other hand, for the second case, the tensor-to-scalar ratio and scalar spectral tilt are constrained within the window,  $0.121 < r < 0.124$  and  $0.969 < n_S < 0.970$ , which is consistent with  $2\sigma$  CL constraints.

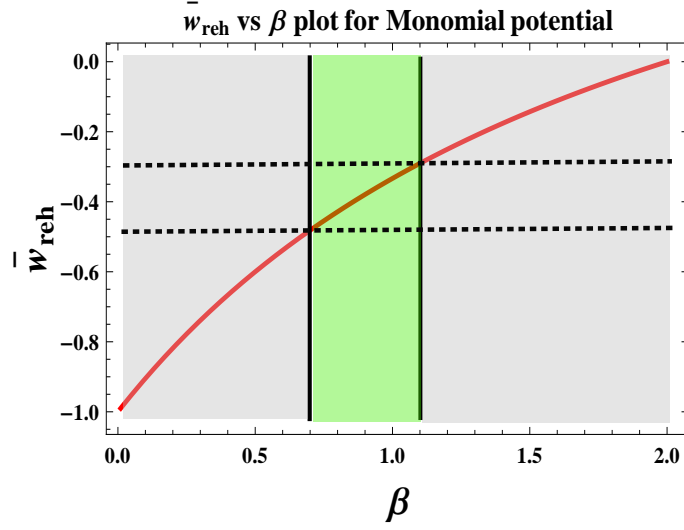


**Figure 6.** Variation of the mean equation of state parameter with respect to the monomial index  $\beta$ . The green shaded region bounded by two vertical black coloured lines and two black coloured horizontal line represent the Planck  $2\sigma$  allowed region and the rest of the light grey shaded region is disfavoured by the Planck data and Planck+ BICEP2+Keck Array joint constraint. It is also observed from the plot that, if we fix the number of e-foldings within the window,  $\Delta\mathcal{N}_b \approx \mathcal{O}(50 - 70)$ , then the mean equation of state parameter  $\bar{w}_{reh}$  is constrained as,  $-0.48 < \bar{w}_{reh} < -0.29$ .

$$\rho_{reh} = \frac{(8.46 \times 10^{-7} M_p^4)}{\left[1 + \left(1 + \frac{2}{\beta}\right) \Delta\mathcal{N}_b\right]} \times \exp\left[\frac{6\beta\Delta\mathcal{N}_b}{\beta + 2}\right] \times \left(\frac{B_0}{\sqrt{2\rho_\gamma}}\right)^{-\frac{\beta}{(\beta-4)}} \quad (6.23)$$

and also using the numerical constraint on the energy density at the end of inflation, as stated in Eq (6.5), I get following stringent constraint on the magnetic field measured at the present epoch in terms of model parameter  $\beta$  for instantaneous reheating<sup>21</sup> as:

$$\frac{(8.68 \times 10^{-6})^{\frac{4-\beta}{\beta}} \left[1 + \left(1 + \frac{2}{\beta}\right) \Delta\mathcal{N}_b\right]^{\frac{4-\beta}{\beta}}}{\exp\left[\frac{6(4-\beta)\Delta\mathcal{N}_b}{\beta+2}\right]} < \frac{B_0}{\sqrt{2\rho_\gamma}} < \frac{(7.02 \times 10^{-4})^{\frac{4-\beta}{\beta}} \left[1 + \left(1 + \frac{2}{\beta}\right) \Delta\mathcal{N}_b\right]^{\frac{4-\beta}{\beta}}}{\exp\left[\frac{6(4-\beta)\Delta\mathcal{N}_b}{\beta+2}\right]}. \quad (6.24)$$

Next using Eq (5.34), I get the following constraint on the dimensionless magnetic density parameter:

$$\Omega_{B_{end}} = \frac{B_0^4 M_p^6}{24\sigma H_0^2 \rho_\gamma^2 \left[1 + \left(1 + \frac{2}{\beta}\right) \Delta\mathcal{N}_b\right]^2} \times (7.16 \times 10^{-13}) \times \exp[8\Delta\mathcal{N}_b]. \quad (6.25)$$

<sup>21</sup>For instantaneous reheating the energy density of inflaton at the end of inflation is instantaneously converted to the reheating energy density or radiation and the instantaneous transition occurs at  $\rho_{end} = \rho_{reh}$ . Commonly this physical situation is known as instantaneous entropy generation scenario [67].

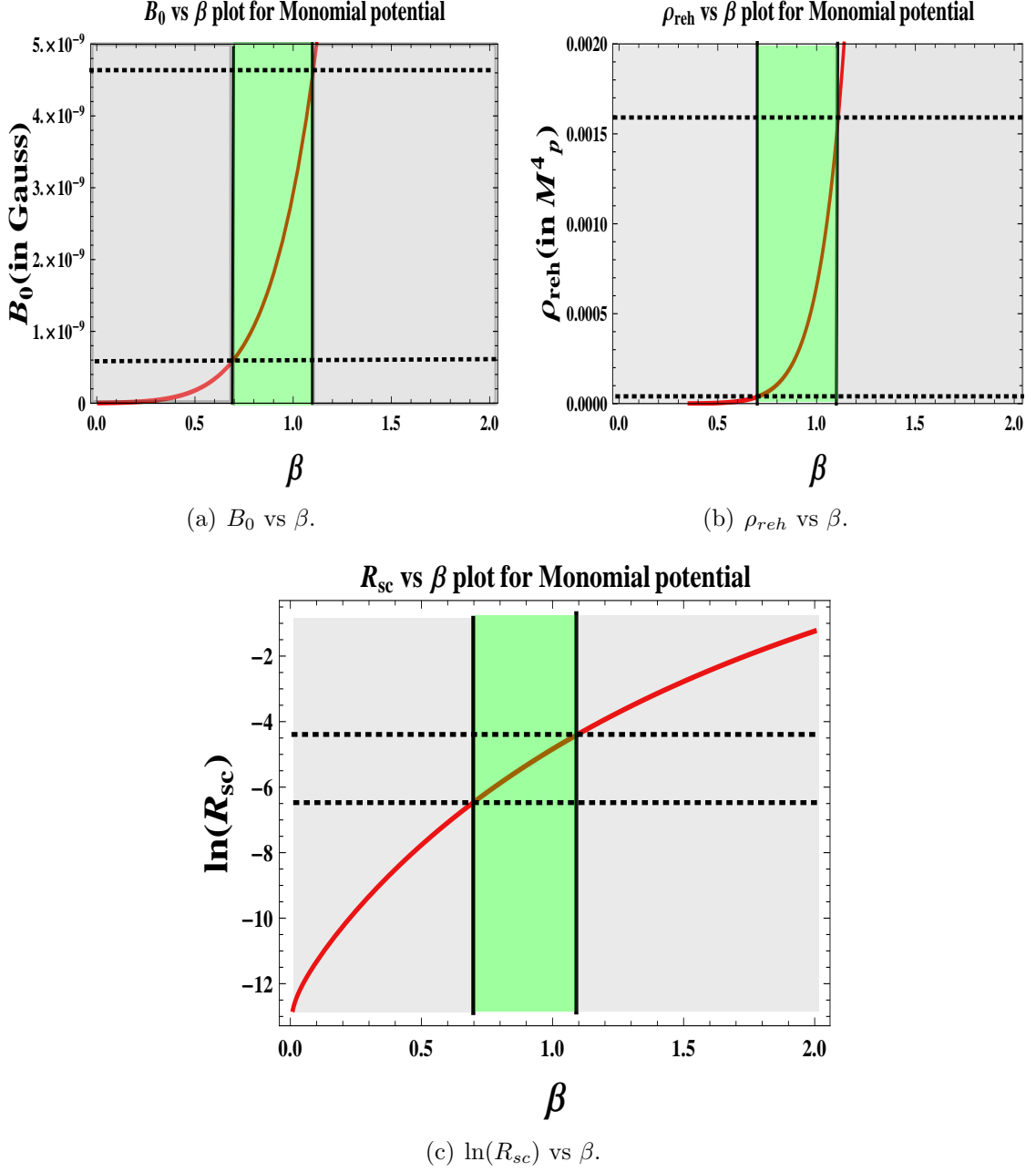
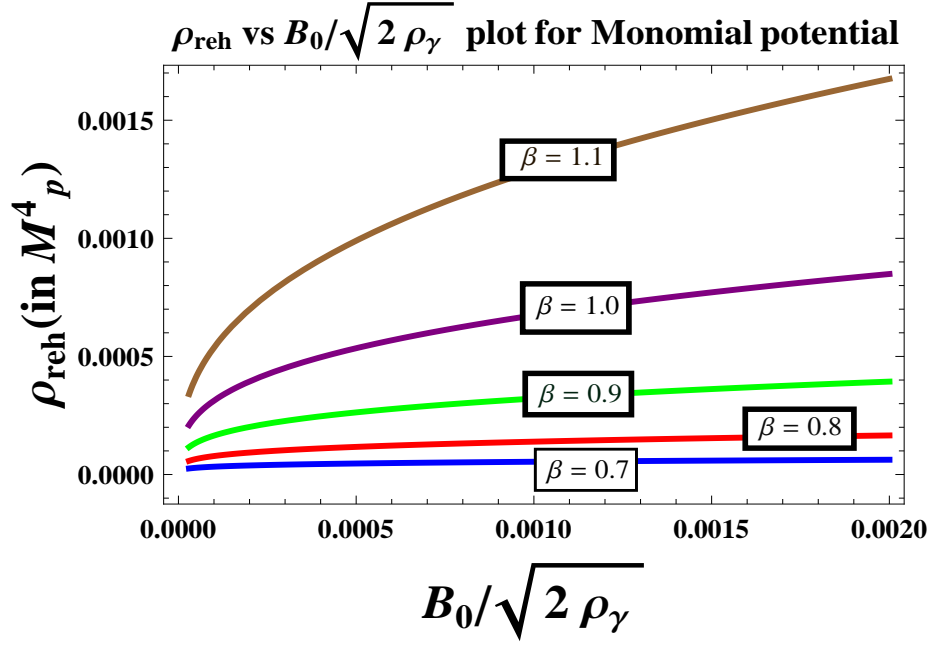
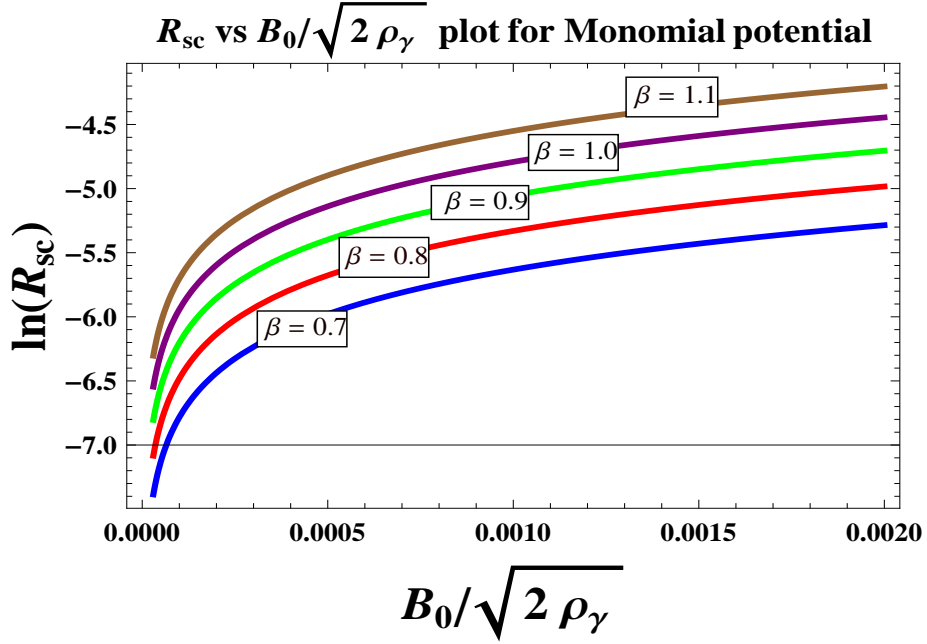


**Figure 7.** Variation of 7(a) the magnetic field at the present epoch  $B_0$ , 7(b) reheating energy density and 7(c) logarithm of reheating characteristic parameter with respect to the characteristic index  $\beta$  of the hilltop potential for  $\Delta\mathcal{N}_b = 50$ ,  $|\Delta\tilde{\mathcal{N}}_b| = 7$  and  $\sigma \sim 5 \times 10^{-16} M_p^4$ . The green shaded region bounded by two vertical black coloured lines and two black coloured horizontal line represent the Planck  $2\sigma$  allowed region and the rest of the light grey shaded region is disfavoured by the Planck data and Planck+ BICEP2+Keck Array joint constraint. In 7(a)-7(c) the black horizontal dotted line correspond to the  $2\sigma$  CL constrained value of the magnetic field at the present epoch, reheating energy density and  $\ln(R_{\text{sc}})$ .





(a)  $\rho_{\text{reh}}$  vs  $B_0/\sqrt{2\rho_\gamma}$ .



(b)  $\ln(R_{\text{sc}})$  vs  $B_0/\sqrt{2\rho_\gamma}$ .

**Figure 8.** Variation of 8(a) the reheating energy density and 8(b) logarithm of reheating characteristic parameter with respect to the scaled magnetic field at the present epoch  $\frac{B_0}{\sqrt{2\rho_\gamma}}$  for the characteristic index  $\beta = 0.7$ (blue),  $0.8$ (red),  $0.9$ (green),  $1.0$ (purple),  $1.1$ (brown). Here we fix  $\Delta\mathcal{N}_b = 50$ ,  $\Delta\tilde{\mathcal{N}}_b = 7$  and  $\sigma \sim 5 \times 10^{-16} M_p^4$ .

Finally the rescaled reheating parameter can be expressed in terms of the model parameters of the monomial models of inflationary potential as:

$$R_{sc} = \frac{3.03 \times 10^{-2}}{\left[1 + \left(1 + \frac{2}{\beta}\right) \Delta \mathcal{N}_b\right]^{1/4}} \times \exp \left[ \frac{3\beta \Delta \bar{\mathcal{N}}_b}{2(\beta + 2)} \right] \times \left( \frac{B_0}{\sqrt{2\rho_\gamma}} \right)^{1/2} \quad (6.26)$$

and using the numerical constraint on the rescaled reheating parameter as stated in Eq (6.4) I get the lower bound on the present value of the magnetic field for the monomial potentials as:

$$\frac{B_0}{\sqrt{2\rho_\gamma}} > \frac{8.6 \times 10^{-23} \times \left[1 + \left(1 + \frac{2}{\beta}\right) \Delta \mathcal{N}_b\right]^{1/2}}{\exp \left[ \frac{3\beta \Delta \bar{\mathcal{N}}_b}{\beta + 2} \right]} \quad (6.27)$$

In fig. 7(a), fig. 7(b) and in fig. 7(c) I have explicitly shown the variation of the magnetic field at the present epoch  $B_0$ , reheating energy density  $\rho_{reh}$  and logarithm of reheating characteristic parameter  $\ln(R_{sc})$  with respect to the characteristic index  $\beta$  of the monomial potential for the number of e-foldings  $\Delta \mathcal{N}_b = 50$ . The green shaded region bounded by two vertical black coloured lines and two black coloured horizontal line represent the Planck  $2\sigma$  allowed region and the rest of the light grey shaded region is disfavoured by the Planck data and Planck+ BICEP2+Keck Array joint constraint. Also in fig. 8(a) and in fig. 8(b) I have depicted the behaviour of the reheating energy density  $\rho_{reh}$  and logarithm of reheating characteristic parameter  $\ln(R_{sc})$ , with respect to the scaled magnetic field at the present epoch  $B_0/\sqrt{2\rho_\gamma}$  for the characteristic index  $0.7 \leq \beta \leq 1.1$ .

Further using Eq (6.12) in Eq (3.30) and Eq (3.37) finally I get the following constraints on the regulating factor within RSII setup as<sup>22</sup>:

$$\Sigma_b(k_L = k_0, k_*) \times \left( \frac{M_p^4}{\sigma} \right)^{2/5} \approx \mathcal{O}(1.58 \times 10^{-21}) \times \left[ 1 + \left( 1 + \frac{2}{\beta} \right) \Delta \mathcal{N}_b \right] \quad (6.29)$$

which is compatible with the observed/measured bound on CP asymmetry and baryon asymmetry parameter.

From fig. 7(a), fig. 7(b) and fig. 7(c) I get the following  $2\sigma$  constraints on magneto

---

<sup>22</sup>After fixing  $\Delta \mathcal{N}_b \approx \mathcal{O}(50 - 70)$ , the regulating factor within RSII can be constrained as,

$$3.06 \times 10^{-19} < \Sigma_b(k_L = k_0, k_*) \times \left( \frac{M_p^4}{\sigma} \right)^{2/5} < 3.13 \times 10^{-19}, \quad (6.28)$$

which is consistent with the upper bound mentioned in Eq (3.33).

reheating cosmological parameters computed from the monomial inflationary model:

$$5.969 \times 10^{-10} \text{ Gauss} < B_0 = \sqrt{\frac{I_\xi(k_L=k_0, k_\Lambda)}{2\pi^2}} A_{\mathbf{B}} < 4.638 \times 10^{-9} \text{ Gauss}, \quad (6.30)$$

$$1.940 \times 10^{-132} M_p^4 < \rho_{B_0} = B_0^2/2 < 1.171 \times 10^{-130} M_p^4, \quad (6.31)$$

$$4.061 \times 10^{-5} M_p^4 < \rho_{reh} < 1.591 \times 10^{-3} M_p^4, \quad (6.32)$$

$$6.227 \times 10^{-4} \times g_*^{-1/4} M_p < T_{reh} < 4.836 \times 10^{-3} \times g_*^{-1/4} M_p, \quad (6.33)$$

$$\Gamma_{total} \sim 0.24 M_p, \quad (6.34)$$

$$1.55 \times 10^{-3} < R_{sc} < 1.24 \times 10^{-2}, \quad (6.35)$$

$$\epsilon_{\mathbf{CP}} \sim \mathcal{O}(10^{-6}), \quad (6.36)$$

$$\eta_B \sim \mathcal{O}(10^{-9}), \quad (6.37)$$

$$0.121 < r < 0.124, \quad (6.38)$$

$$0.969 < n_S < 0.970, \quad (6.39)$$

$$2.3794 \times 10^{-9} < P_S < 2.3798 \times 10^{-9}, \quad (6.40)$$

$$8.08 \times 10^{-3} M_p < \sqrt[4]{V_0} < 8.13 \times 10^{-3} M_p, \quad (6.41)$$

for the number of e-foldings  $\Delta\mathcal{N}_b = 50$ ,  $|\Delta\bar{\mathcal{N}}_b| = 7$ , mean equation of state parameter  $-0.48 < \bar{w}_{reh} < -0.29$  and  $\Omega_{rad} h^2 \sim 2.5 \times 10^{-5}$ , alongwith the following restricted model parameter space:

$$0.7 < \beta < 1.1, \quad (6.42)$$

$$\sigma \sim 5 \times 10^{-16} M_p^4, \quad (6.43)$$

$$M_5 \sim \left( 1.042 \times 10^{-32} \times \frac{M_p^8}{|\tilde{\Lambda}_5|} \right)^{1/3}. \quad (6.44)$$

It is important to note that, if we choose different parameter space by allowing fine tuning in-(1) the energy scale of monomial potential  $V_0 = M^4$ , (2) the brane tension  $\sigma$  and (3) the characteristic index of the monomial potential  $\beta$  then the overall analysis and the obtained results suggests that-

- For  $\beta < 0.7$ , the amplitude of the scalar power spectrum  $P_S$  match the Planck 2015 data and also consistent with the joint constraint obtained from Planck +BICEP2 +Keck Array. But the allowed range for scalar spectral tilt  $n_S$  is outside the observational window. Also in this regime the value of tensor-to-scalar ratio  $r$  is lower compared to the upper bound i.e.  $r \ll 0.12$ . On the other hand, for very low  $\beta$  the estimated value of the magnetic field at the present epoch  $B_0$  from the monomial model is very very small and can reach upto the lower bound  $B_0 > 10^{-15}$  Gauss. Similarly for low  $\beta$ , the reheating energy density  $\rho_{reh}$  or equivalently the reheating temperature  $T_{reh}$  falls down and also the rescaled reheating parameter  $R_{sc}$  decrease.
- For  $1.1 < \beta < 1.2$ , both the amplitude of the scalar power spectrum  $P_S$  and the scalar spectral tilt  $n_S$  are perfectly consistent with the Planck 2015 data and

also consistent with the joint constraint obtained from Planck+BICEP2+Keck Array. But for  $\beta > 1.2$  the estimated value of the amplitude of the scalar power spectrum falls down from its predicted bound from observation. Also for  $\beta > 1.2$  region the value of tensor-to-scalar ratio  $r$  is very very large compared to its the upper bound i.e.  $r \gg 0.12$ . As  $\beta$  increases the estimated value of the magnetic field at the present epoch  $B_0$  exceeds the upper bound i.e.  $B_0 \gg 10^{-9}$  Gauss as obtained from Faraday rotation. Additionally in the large  $\beta$  regime the reheating energy density  $\rho_{reh}$  or equivalently the reheating temperature  $T_{reh}$  and the rescaled reheating parameter  $R_{sc}$  are not consistent with the observational constraints.

## 6.2 Hilltop Models

In case of hilltop models the inflationary potential can be represented by the following functional form:

$$V(\phi) = V_0 \left[ 1 - \left( \frac{\phi}{\mu} \right)^\beta \right] \quad (6.45)$$

where  $V_0 = M^4$  is the tunable energy scale, which is necessarily required to fix the amplitude of the CMB anisotropies and  $\beta$  is the characteristic index which characterizes the feature of the potential. In the present context  $V_0$  mimics the role of vacuum energy and the scale of inflation is fixed by this correction term. The variation of the hilltop potential for the index  $\beta = 2, 4, 6$ , mass parameter  $\mu = 0.1 M_p, 1 M_p, 10 M_p$  and the tunable scale  $\sqrt[4]{V_0} = 4.12 \times 10^{-3} M_p = 10^{16} \text{ GeV}$  is shown in fig. 9(a), fig. 9(b) and fig. 9(c) respectively. To analyze the detailed features of the hilltop potential here I start with the definition of number of e-foldings  $\Delta\mathcal{N}_b(\phi)$  in the high energy regime of RSII setup (see Appendix 8.1 for details), using which I get:

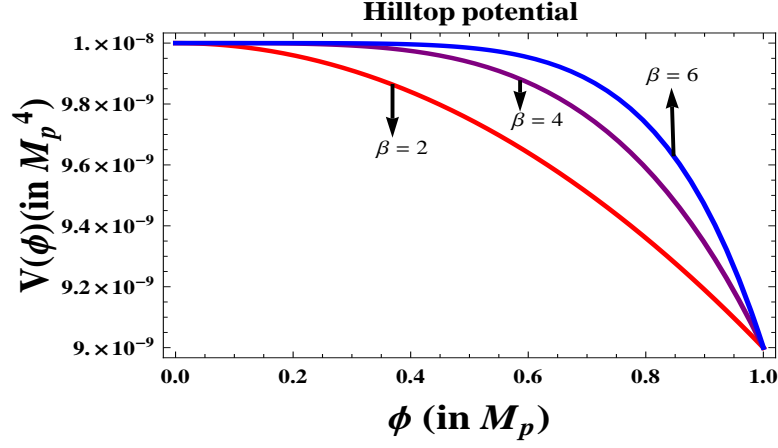
$$\Delta\mathcal{N}_b(\phi) \approx \frac{V_0 \mu^p}{2\sigma\beta(\beta-2)M_p^2} \left( \phi^{2-\beta} - \phi_{end}^{2-\beta} \right). \quad (6.46)$$

Further setting  $\phi = \phi_{cmb}$  in Eq (6.46), the field value at the horizon crossing can be computed as:

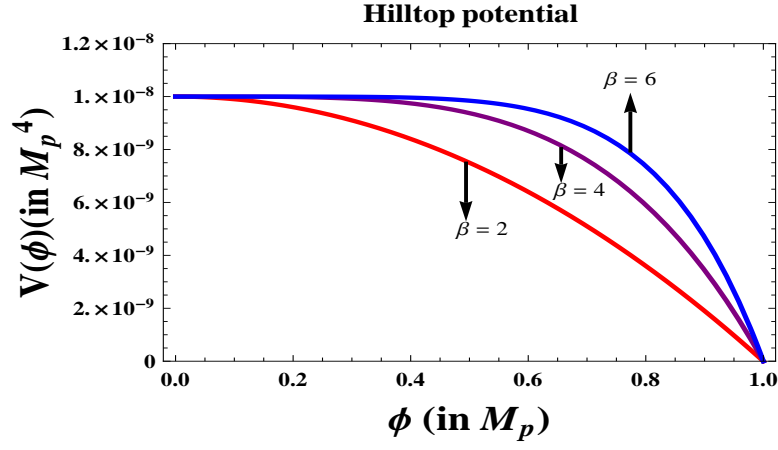
$$\phi_{cmb} \approx \phi_{end} \left[ 1 + \frac{2\sigma\beta(\beta-2)M_p^2\Delta\mathcal{N}_b}{\phi_{end}^{2-\beta}\mu^\beta V_0} \right]^{\frac{1}{2-\beta}} \quad (6.47)$$

where  $\phi_{end}$  represents the field value of inflaton at the end of inflation. Within RSII setup from the violation of the slow-roll conditions one can compute:

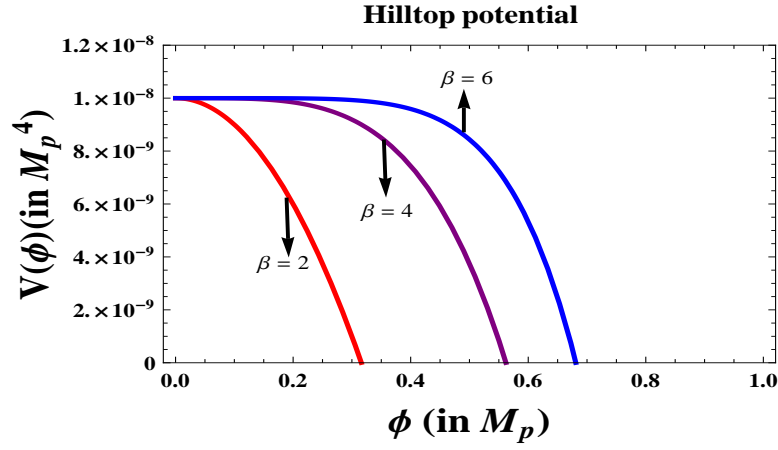
$$\phi_{end} \approx \left( \frac{V_0}{2\sigma\beta^2} \right)^{\frac{1}{2(\beta-1)}} \left( \frac{\mu}{M_p} \right)^{\frac{\beta}{\beta-1}} M_p. \quad (6.48)$$



(a) For  $\mu = 10 M_p$ .



(b) For  $\mu = 1 M_p$ .



(c) For  $\mu = 0.1 M_p$ .

**Figure 9.** Variation of the hilltop potential for the index  $\beta = 2, 4, 6$ . Here I fix the tunable scale at  $\sqrt[4]{V_0} = 4.12 \times 10^{-3} M_p = 10^{16} \text{ GeV}$ .

From hilltop models of inflation the scale of the potential at the horizon crossing and at the end of inflation can be computed as:

$$\begin{aligned}\rho_{cmb} &\approx V(\phi_{cmb}) = V_0 \left[ 1 - \left( \frac{\phi_{cmb}}{\mu} \right)^\beta \right] \\ &= V_0 \left[ 1 - \left( \frac{V_0}{2\sigma\beta^2} \right)^{\frac{\beta}{2(\beta-1)}} \left( \frac{\mu}{M_p} \right)^{\frac{\beta}{\beta-1}} \left\{ 1 + \frac{2\sigma\beta(\beta-2)M_p^\beta \Delta\mathcal{N}_b}{\left( \frac{V_0}{2\sigma\beta^2} \right)^{\frac{2-\beta}{2(\beta-1)}} \left( \frac{\mu}{M_p} \right)^{\frac{\beta(2-\beta)}{\beta-1}} \mu^\beta V_0} \right\}^{\frac{\beta}{2-\beta}} \right],\end{aligned}\quad (6.49)$$

$$\rho_{end} \approx V(\phi_{end}) = V_0 \left[ 1 - \left( \frac{\phi_{end}}{\mu} \right)^\beta \right] = V_0 \left[ 1 - \left( \frac{V_0}{2\sigma\beta^2} \right)^{\frac{\beta}{2(\beta-1)}} \left( \frac{\mu}{M_p} \right)^{\frac{\beta}{\beta-1}} \right]. \quad (6.50)$$

Further using the consistency condition in the high energy regime of RSII braneworld, as stated in Eq (8.2) of the Appendix 8.1, one can derive the following expressions for the tensor to scalar ratio and scalar spectral tilt as:

$$P_S(k_*) = \frac{V_0 \left[ 1 - \left( \frac{V_0}{2\sigma\beta^2} \right)^{\frac{\beta}{2(\beta-1)}} \left( \frac{\mu}{M_p} \right)^{\frac{\beta}{\beta-1}} \left\{ 1 + \frac{2\sigma\beta(\beta-2)M_p^\beta \Delta\mathcal{N}_b}{\left( \frac{V_0}{2\sigma\beta^2} \right)^{\frac{2-\beta}{2(\beta-1)}} \left( \frac{\mu}{M_p} \right)^{\frac{\beta(2-\beta)}{\beta-1}} \mu^\beta V_0} \right\}^{\frac{\beta}{2-\beta}} \right]}{36\pi^2 \left\{ 1 + \frac{2\sigma\beta(\beta-2)\Delta\mathcal{N}_b}{\left( \frac{V_0}{2\sigma\beta^2} \right)^{\frac{2-\beta}{2(\beta-1)}} \left( \frac{\mu}{M_p} \right)^{\frac{\beta}{\beta-1}} V_0} \right\}^{\frac{2(\beta-1)}{2-\beta}}}}, \quad (6.51)$$

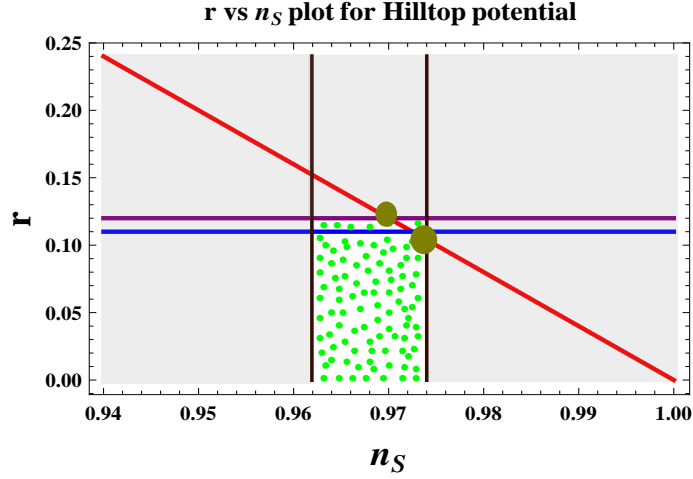
$$r(k_*) = 24 \left\{ 1 + \frac{2\sigma\beta(\beta-2)\Delta\mathcal{N}_b}{\left( \frac{V_0}{2\sigma\beta^2} \right)^{\frac{2-\beta}{2(\beta-1)}} \left( \frac{\mu}{M_p} \right)^{\frac{\beta}{\beta-1}} V_0} \right\}^{\frac{2(\beta-1)}{2-\beta}}, \quad (6.52)$$

$$n_S(k_*) - 1 \approx -6 \left\{ 1 + \frac{2\sigma\beta(\beta-2)\Delta\mathcal{N}_b}{\left( \frac{V_0}{2\sigma\beta^2} \right)^{\frac{2-\beta}{2(\beta-1)}} \left( \frac{\mu}{M_p} \right)^{\frac{\beta}{\beta-1}} V_0} \right\}^{\frac{2(\beta-1)}{2-\beta}}. \quad (6.53)$$

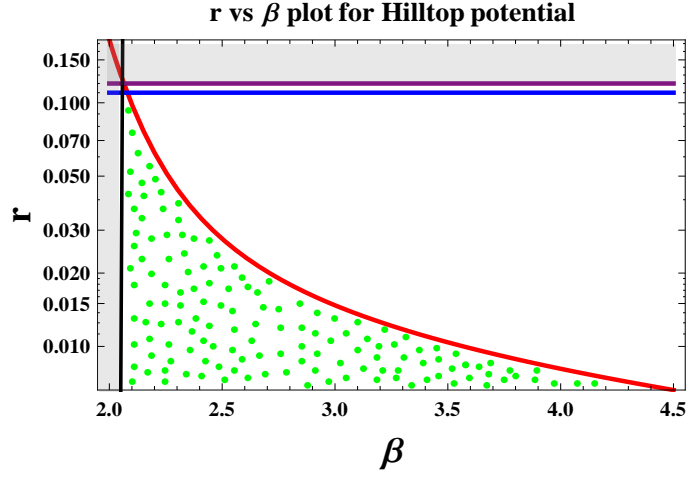
and to satisfy the joint constraint on the scalar spectral tilt and upper bound of tensor-to-scalar ratio as observed by Planck (2013 and 2015) and Planck+BICEP2+Keck Array, one need the following constraint on the parameters of the inflationary potential:

$$\frac{2\sigma\Delta\mathcal{N}_b}{V_0} < \frac{\exp \left[ \frac{2.65(\beta-2)}{(\beta-1)} \right] - 1}{\beta(\beta-2)} \left( \frac{V_0}{2\sigma\beta^2} \right)^{\frac{2-\beta}{2(\beta-1)}} \left( \frac{\mu}{M_p} \right)^{\frac{\beta}{\beta-1}}. \quad (6.54)$$

The behaviour of the tensor-to-scalar ratio  $r$  with respect to the scalar spectral index  $n_S$  and the characteristic parameter of the hilltop potential  $\beta$  are plotted in fig. 10(a) and fig. 10(b) respectively. From 10(a) it is observed that, within  $50 < \Delta\mathcal{N}_b < 70$  the



(a)  $r$  vs  $n_S$ .



(b)  $r$  vs  $\beta$ .

**Figure 10.** Behaviour of the tensor-to-scalar ratio  $r$  with respect to **10(a)** the scalar spectral index  $n_S$  and **10(b)** the characteristic parameter of the hilltop potential  $\beta$  for the brane tension  $\sigma \sim 10^{-9} M_p^4$  and the mass scale parameter  $\mu = 5.17 M_p$ . The purple and blue coloured line represent the upper bound of tensor-to-scalar ratio allowed by Planck+ BICEP2+Keck Array joint constraint and only Planck 2015 data respectively. The small and the big bubbles represent two consecutive points in  $r - n_S$  plane, where for the small bubble  $\Delta\mathcal{N}_b = 50, r = 0.124, n_S = 0.969$  and for the big bubble  $\Delta\mathcal{N}_b = 70, r = 0.121, n_S = 0.970$  respectively. In **10(a)** and **10(b)** the green dotted region signifies the Planck  $2\sigma$  allowed region and the rest of the light grey shaded region is excluded by the Planck data and Planck+ BICEP2+Keck Array joint constraint. From **10(a)** it is observed that, within  $50 < \Delta\mathcal{N}_b < 70$  the hilltop potential is favoured for the characteristic index  $\beta > 2.04$ , by Planck 2015 data and Planck+ BICEP2+Keck Array joint analysis. In **10(b)** I have explicitly shown that the in  $r - \beta$  plane the observationally favoured lower bound for the characteristic index of the hilltop potential is  $\beta > 2.04$ .

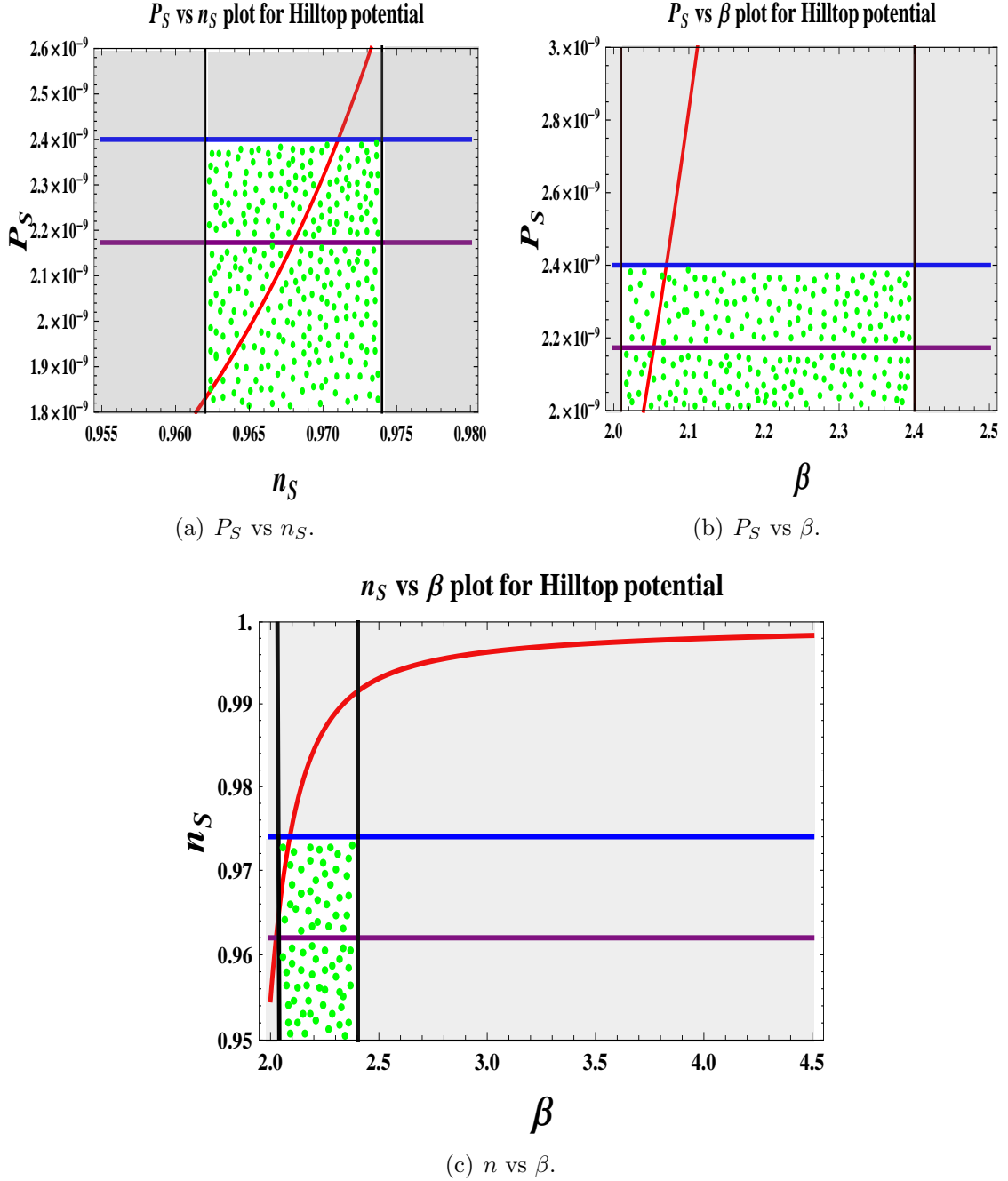


**Figure 11.** Variation of the 11(a) scalar power spectrum  $P_S$  vs scalar spectral index  $n_S$ , 11(b) scalar power spectrum  $P_S$  vs index  $\beta$  and 11(c) scalar power spectrum  $n_S$  vs index  $\beta$ . The purple and blue coloured line represent the upper and lower bound allowed by WMAP+Planck 2015 data respectively. The green dotted region bounded by two vertical black coloured lines represent the Planck  $2\sigma$  allowed region and the rest of the light grey shaded region is disfavoured by the Planck+WMAP constraint.

hilltop potential is favoured for the characteristic index  $\beta > 2.04$ , by Planck 2015 data



and Planck+ BICEP2+Keck Array joint analysis. In 10(b) I have explicitly shown that the in  $r - \beta$  plane the observationally favoured window for the characteristic index is  $\beta > 2.04$ . Additionally it is important to note that, for hilltop potentials embedded in the high energy regime of RSII braneworld, the consistency relation between tensor-to-scalar ratio  $r$  and the scalar spectral  $n_S$  is given by,

$$r \approx 4(1 - n_S). \quad (6.55)$$

On the other hand in the low energy regime of RSII braneworld or equivalently in the GR limiting situation, the consistency relation between tensor-to-scalar ratio  $r$  and the scalar spectral  $n_S$  is modified as,

$$r \approx \frac{8}{3}(1 - n_S). \quad (6.56)$$

This also clearly suggests that the estimated numerical value of the tensor-to-scalar ratio from the GR limit is different compared to its value in the high density regime of the RSII braneworld. To justify the validity of this statement, let me discuss a very simplest situation, where the scalar spectral index is constrained within  $0.969 < n_S < 0.970$ , as appearing in this paper. Now in such a case using the consistency relation in GR limit one can easily compute that the tensor-to-scalar is constrained within the window,  $0.080 < r < 0.083$ , which is pretty consistent with Planck 2015 result.

Variation of the 11(a) scalar power spectrum  $P_S$  vs scalar spectral index  $n_S$ , 11(b) scalar power spectrum  $P_S$  vs index  $\beta$  and 11(c) scalar power spectrum  $n_S$  vs index  $\beta$ . The purple and blue coloured line represent the upper and lower bound allowed by WMAP+Planck 2015 data respectively. The green dotted region bounded by two vertical black coloured lines represent the Planck  $2\sigma$  allowed region and the rest of the light grey shaded region is disfavoured by the Planck+WMAP constraint. From the fig. 11(a)-fig. 11(c) it is clearly observed that the characteristic index of the the inflationary potential is constrained within the window  $2.04 < \beta < 2.4$  for the amplitude of the scalar power spectrum,  $2.3794 \times 10^{-9} < P_S < 2.3798 \times 10^{-9}$  and scalar spectral tilt,  $0.969 < n_S < 0.970$ . Now using Eq (6.51), Eq (6.52) and Eq (6.53) one can write another consistency relation among the amplitude of the scalar power spectrum  $P_S$ , tensor-to-scalar ratio  $r$  and scalar spectral index  $n_S$  for hilltop potentials embedded in the high density regime of RSII braneworld as:

$$\begin{aligned} P_S &= \frac{V_0 \left[ 1 - \left( \frac{V_0}{2\sigma\beta^2} \right)^{\frac{\beta}{2(\beta-1)}} \left( \frac{\mu}{M_p} \right)^{\frac{\beta}{\beta-1}} \left( \frac{1-n_S}{6} \right)^{\frac{\beta}{2(\beta-1)}} \right]}{6\pi^2(1 - n_S)} \\ &= \frac{2V_0 \left[ 1 - \left( \frac{V_0}{2\sigma\beta^2} \right)^{\frac{\beta}{2(\beta-1)}} \left( \frac{\mu}{M_p} \right)^{\frac{\beta}{\beta-1}} \left( \frac{r}{24} \right)^{\frac{\beta}{2(\beta-1)}} \right]}{3\pi^2 r}. \end{aligned} \quad (6.57)$$

Further using Eq (3.21), I get the following stringent constraint on the tunable energy scale of the hilltop models of inflation:

$$V_0 = M^4 < 5.98 \times 10^{-8} M_p^4. \quad (6.58)$$

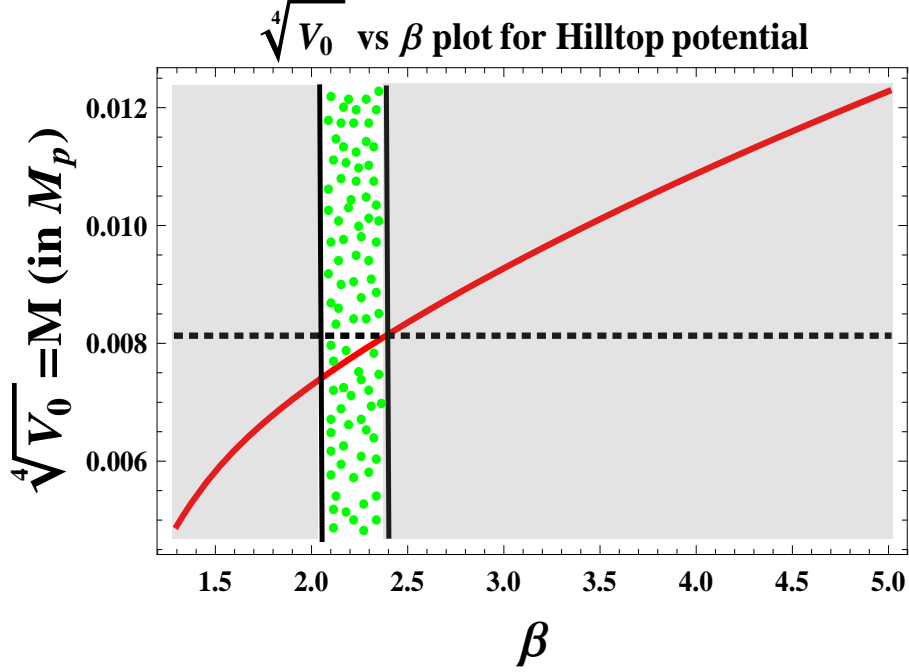


**Figure 12.** Variation of the energy scale of the hilltop potential with respect to the characteristic index  $\beta$  for the brane tension  $\sigma \sim 10^{-9} M_p^4$  and the mass scale parameter  $\mu = M_p$ . The green dotted region bounded by two vertical black coloured lines and one black coloured horizontal line represent the Planck  $2\sigma$  allowed region and the rest of the light grey shaded region is disfavoured by the Planck data and Planck+ BICEP2+Keck Array joint constraint. This analysis explicitly shows that the  $2\sigma$  allowed window for the parameter  $\beta$  within  $2.04 < \beta < 2.4$  constraints the scale of inflation within  $8.08 \times 10^{-3} M_p < \sqrt[4]{V_0} < 8.13 \times 10^{-3} M_p$ . Here for  $\sigma \sim 10^{-9} M_p^4$  the tensor-to-scalar ratio and scalar spectral tilt are constrained within the window,  $0.121 < r < 0.124$  and  $0.969 < n_S < 0.970$ , which is consistent with  $2\sigma$  CL constraints.

The variation of the energy scale of the hilltop potential with respect to the characteristic index  $\beta$  for the brane tension  $\sigma \sim 10^{-9} M_p^4$  and the mass scale parameter  $\mu = M_p$  is shown in fig. 12. This analysis explicitly shows that for  $\sigma \sim 10^{-9} M_p^4$  the tensor-to-scalar ratio and scalar spectral tilt are constrained within the window,  $0.121 < r < 0.124$  and  $0.969 < n_S < 0.970$ , which is consistent with  $2\sigma$  CL constraints.

Further using Eq (5.20) and Eq (5.21) the reheating energy density can be com-

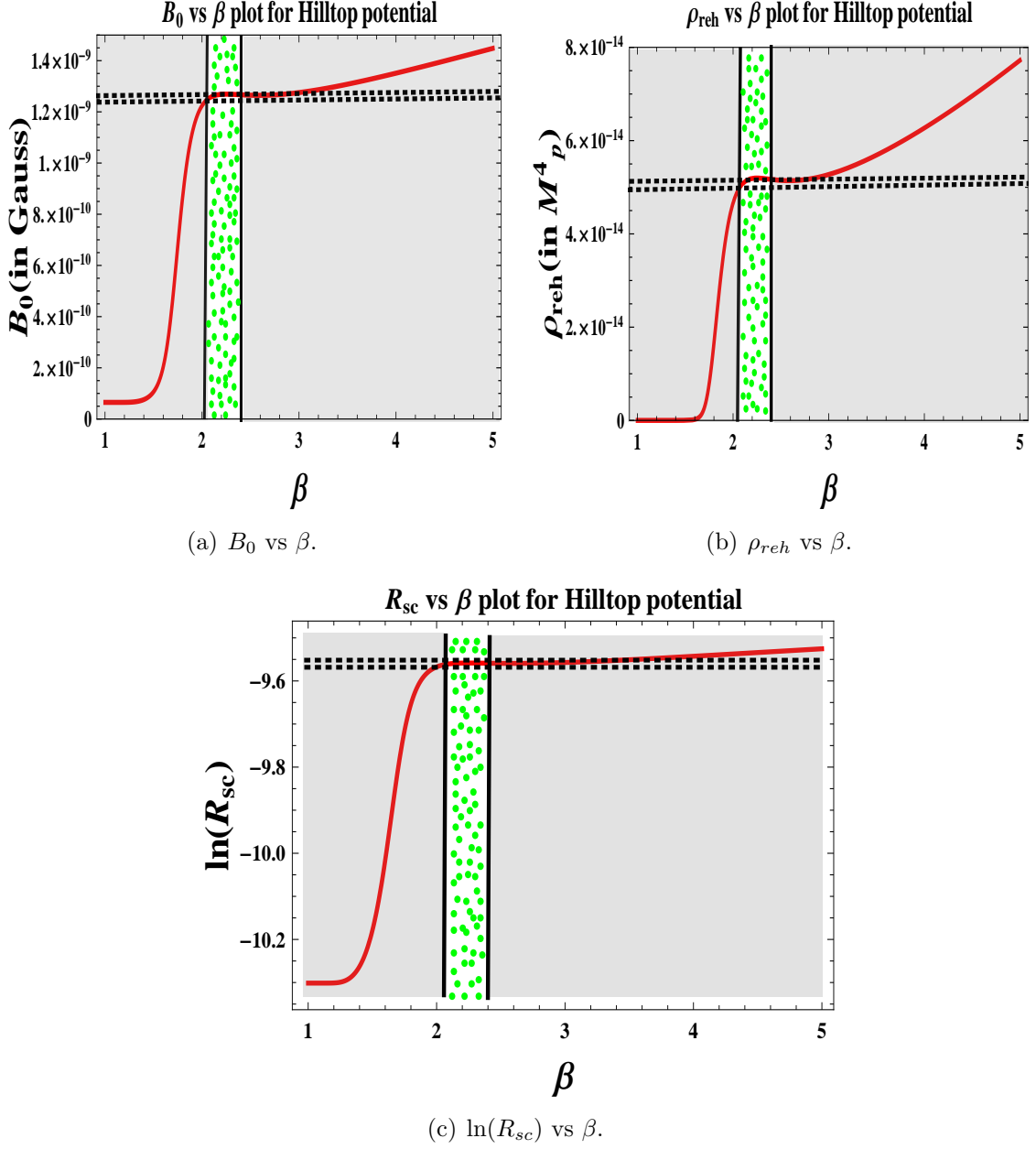
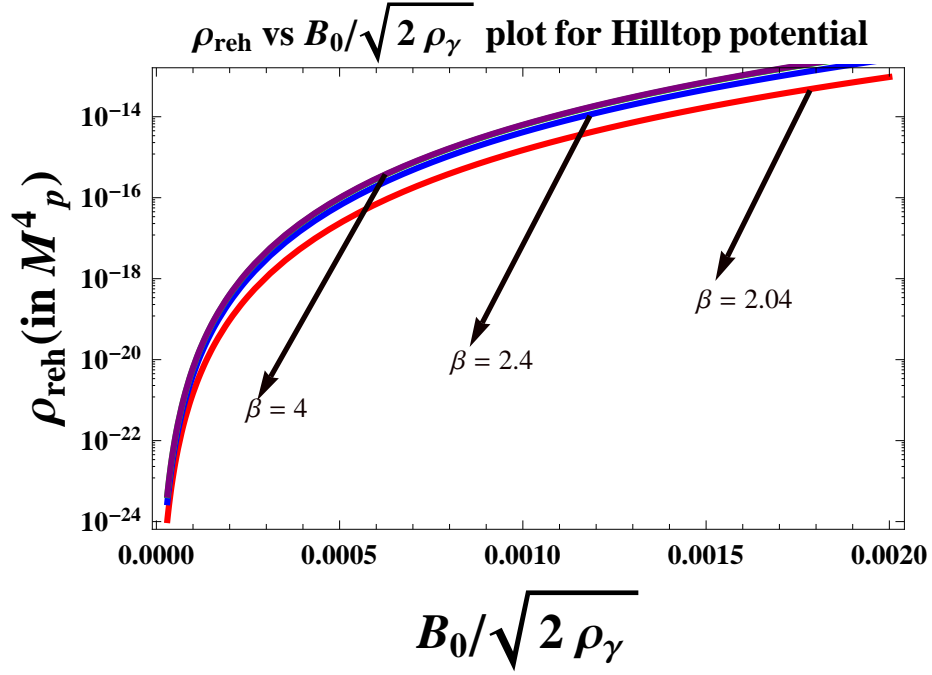
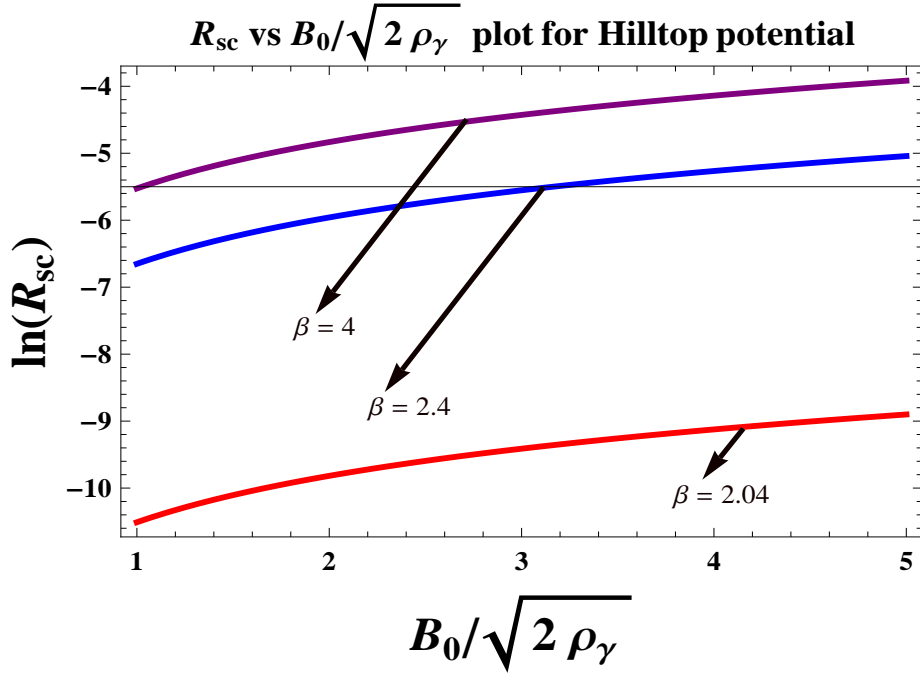


**Figure 13.** Variation of **13(a)** the magnetic field at the present epoch  $B_0$ , **13(b)** reheating energy density and **13(c)** logarithm of reheating characteristic parameter with respect to the characteristic index  $\beta$  of the hilltop potential for  $\Delta\mathcal{N}_b = 50$ ,  $|\Delta\mathcal{N}_b| = 11.5$ ,  $\sigma \sim 10^{-9} M_p^4$ ,  $\mu = 1 M_p$  and  $\bar{w}_{reh} = 0$ . The green dotted region bounded by two vertical black coloured lines and two black coloured horizontal line represent the Planck  $2\sigma$  allowed region and the rest of the light grey shaded region is disfavoured by the Planck data and Planck+ BICEP2+Keck Array joint constraint. In **13(a)-13(c)** the black horizontal dotted line correspond to the  $2\sigma$  CL constrained value of the magnetic field at the present epoch, reheating energy density and  $\ln(R_{sc})$ .



(a)  $\rho_{\text{reh}}$  vs  $B_0/\sqrt{2\rho_\gamma}$ .



(b)  $\ln(R_{\text{sc}})$  vs  $B_0/\sqrt{2\rho_\gamma}$ .

**Figure 14.** Variation of 14(a) the reheating energy density and 14(b) logarithm of reheating characteristic parameter with respect to the scaled magnetic field at the present epoch  $\frac{B_0}{\sqrt{2\rho_\gamma}}$  for the characteristic index  $\beta = 2.04$ (red),  $2.4$ (blue),  $4$ (purple).

puted as:

$$\rho_{reh} \geq (8.46 \times 10^{-7} M_p^4) \times \left\{ 1 + \frac{2\sigma\beta(\beta-2)\Delta\mathcal{N}_b}{\left(\frac{V_0}{2\sigma\beta^2}\right)^{\frac{2-\beta}{2(\beta-1)}} \left(\frac{\mu}{M_p}\right)^{\frac{\beta}{\beta-1}} V_0} \right\}^{\frac{2(\beta-1)}{2-\beta}} \times \begin{cases} \exp[3\Delta\bar{\mathcal{N}}_b] \times \left(\frac{B_0}{\sqrt{2\rho_\gamma}}\right)^6 & \text{for } \bar{w}_{reh} = 0 \\ \exp[4\Delta\bar{\mathcal{N}}_b] \left(\frac{B_0}{\sqrt{2\rho_\gamma}}\right)^{-\frac{4\Delta\bar{\mathcal{N}}_b}{\ln\left(\frac{B_0}{\sqrt{2\rho_\gamma}}\right)}} & \text{for } \bar{w}_{reh} \neq 0. \end{cases} \quad (6.59)$$

Next using Eq (5.34), I get the following constraint on the dimensionless magnetic density parameter:

$$\Omega_{B_{end}} = \frac{B_0^4 M_p^6}{24\sigma H_0^2 \rho_\gamma^2} \times (7.16 \times 10^{-13}) \times \left\{ 1 + \frac{2\sigma\beta(\beta-2)\Delta\mathcal{N}_b}{\left(\frac{V_0}{2\sigma\beta^2}\right)^{\frac{2-\beta}{2(\beta-1)}} \left(\frac{\mu}{M_p}\right)^{\frac{\beta}{\beta-1}} V_0} \right\}^{\frac{4(\beta-1)}{2-\beta}} \times \exp[8\Delta\bar{\mathcal{N}}_b]. \quad (6.60)$$

Finally the rescaled reheating parameter can be expressed in terms of the model parameters of the hilltop models of inflationary potential as <sup>23</sup>:

$$R_{sc} = 3.03 \times 10^{-2} \times \left\{ 1 + \frac{2\sigma\beta(\beta-2)\Delta\mathcal{N}_b}{\left(\frac{V_0}{2\sigma\beta^2}\right)^{\frac{2-\beta}{2(\beta-1)}} \left(\frac{\mu}{M_p}\right)^{\frac{\beta}{\beta-1}} V_0} \right\}^{\frac{\beta-1}{2(2-\beta)}} \exp[\Delta\bar{\mathcal{N}}_b] \times \left(\frac{B_0}{\sqrt{2\rho_\gamma}}\right). \quad (6.62)$$

and using the numerical constraint on the rescaled reheating parameter as stated in Eq (6.61) I get the lower bound on the present value of the magnetic field as:

$$\frac{B_0}{\sqrt{2\rho_\gamma}} > \frac{4.45 \times 10^{-12} \times \left\{ 1 + \frac{2\sigma\beta(\beta-2)\Delta\mathcal{N}_b}{\left(\frac{V_0}{2\sigma\beta^2}\right)^{\frac{2-\beta}{2(\beta-1)}} \left(\frac{\mu}{M_p}\right)^{\frac{\beta}{\beta-1}} V_0} \right\}^{\frac{2(\beta-1)}{3(\beta-2)}}}{\exp\left[\frac{4}{3}\Delta\bar{\mathcal{N}}_b\right]}. \quad (6.63)$$

In fig. 13(a), fig. 13(b) and fig. 13(c) I have explicitly shown the variation of the magnetic field at the present epoch  $B_0$ , reheating energy density  $\rho_{reh}$  and logarithm

---

<sup>23</sup>The CMB constraint on the lower bound of the rescaled reheating parameter for hiltop models within  $2\sigma$  CL is given by [73]:

$$R_{sc} > 9.29 \times 10^{-11}. \quad (6.61)$$

of reheating characteristic parameter  $\ln(R_{sc})$  with respect to the characteristic index  $\beta$  of the hilltop potential for the number of e-foldings  $\Delta\mathcal{N}_b = 50$ ,  $|\Delta\bar{\mathcal{N}}_b| = 11.5$ , brane tension  $\sigma \sim 10^{-9} M_p^4$ , mass scale parameter  $\mu = 1 M_p$  and mean equation of state parameter  $\bar{w}_{reh} = 0$ . The green dotted region bounded by two vertical black coloured lines and two black coloured horizontal lines represent the Planck  $2\sigma$  allowed region and the rest of the light grey shaded region is disfavoured by the Planck data and Planck+ BICEP2+Keck Array joint constraint. Also in fig. 14(a) and in fig. 14(b) I have depicted the behaviour of the reheating energy density  $\rho_{reh}$  and logarithm of reheating characteristic parameter  $\ln(R_{sc})$ , with respect to the scaled magnetic field at the present epoch  $B_0/\sqrt{2\rho_\gamma}$  for the characteristic index  $2.04 \leq \beta \leq 2.4$ .

Using Eq (6.52) in Eq (3.30) and Eq (3.37), finally I get the following constraints on the magnetic regulating factor within RSII setup as <sup>24</sup>:

$$\Sigma_b(k_L = k_0, k_*) \times \left(\frac{M_p^4}{\sigma}\right)^{2/5} \approx \mathcal{O}(1.99 \times 10^{-21}) \times \left\{ 1 + \frac{2\sigma\beta(\beta-2)\Delta\mathcal{N}_b}{\left(\frac{V_0}{2\sigma\beta^2}\right)^{\frac{2-\beta}{2(\beta-1)}} \left(\frac{\mu}{M_p}\right)^{\frac{\beta}{\beta-1}} V_0} \right\}^{\frac{2(\beta-1)}{\beta-2}} \quad (6.65)$$

which is compatible with the observed/measured bound on CP asymmetry and baryon asymmetry parameter.

From fig. 10(a)-fig. 13(c), I get the following  $2\sigma$  constraints on cosmological parameters computed from the hilltop inflationary model:

$$1.238 \times 10^{-9} \text{ Gauss} < B_0 = \sqrt{\frac{I_\xi(k_L=k_0, k_\Lambda)}{2\pi^2}} A_{\mathbf{B}} < 1.263 \times 10^{-9} \text{ Gauss}, \quad (6.66)$$

$$8.345 \times 10^{-132} M_p^4 < \rho_{B_0} = B_0^2/2 < 8.685 \times 10^{-132} M_p^4, \quad (6.67)$$

$$4.945 \times 10^{-14} M_p^4 < \rho_{reh} < 5.128 \times 10^{-14} M_p^4, \quad (6.68)$$

$$6.227 \times 10^{-4} \times g_*^{-1/4} M_p < T_{reh} < 6.283 \times 10^{-4} \times g_*^{-1/4} M_p, \quad (6.69)$$

$$\Gamma_{total} \sim 1.7 \times 10^{-4} M_p, \quad (6.70)$$

$$7 \times 10^{-5} < R_{sc} < 7.11 \times 10^{-5}, \quad (6.71)$$

$$\epsilon_{\mathbf{CP}} \sim \mathcal{O}(10^{-6}), \quad (6.72)$$

$$\eta_B \sim \mathcal{O}(10^{-9}), \quad (6.73)$$

$$0.121 < r < 0.124, \quad (6.74)$$

$$0.969 < n_S < 0.970, \quad (6.75)$$

$$2.3794 \times 10^{-9} < P_S < 2.3798 \times 10^{-9}, \quad (6.76)$$

$$8.08 \times 10^{-3} M_p < \sqrt[4]{V_0} < 8.13 \times 10^{-3} M_p, \quad (6.77)$$

---

<sup>24</sup>After fixing  $\Delta\mathcal{N}_b \approx \mathcal{O}(50 - 70)$ , the regulating factor within RSII can be constrained as,

$$\Sigma_b(k_L = k_0, k_*) \times \left(\frac{M_p^4}{\sigma}\right)^{2/5} < 3.98 \times 10^{-19}, \quad (6.64)$$

which is consistent with the upper bound mentioned in Eq (3.33).

for the number of e-foldings  $\Delta\mathcal{N}_b = 50$ ,  $|\Delta\tilde{\mathcal{N}}_b| = 11.5$ , mean equation of state parameter  $\bar{w}_{reh} = 0$  and  $\Omega_{rad}h^2 \sim 2.5 \times 10^{-5}$ , alongwith the following restricted model parameter space:

$$2.04 < \beta < 2.4, \quad (6.78)$$

$$\mu \sim \mathcal{O}(M_p), \quad (6.79)$$

$$\sigma \sim 10^{-9} M_p^4, \quad (6.80)$$

$$M_5 \sim \left( 4.170 \times 10^{-20} \times \frac{M_p^8}{|\tilde{\Lambda}_5|} \right)^{1/3}. \quad (6.81)$$

It is important to mention here that, if we choose different parameter space by allowing fine tuning in-(1) the energy scale of hilltop potential  $V_0 = M^4$ , (2) the mass scale parameter  $\mu$  of the hilltop model, (3) the brane tension  $\sigma$  and (4) the characteristic index of the hilltop potential  $\beta$  then the overall analysis and the obtained results suggests that-

- For  $\beta < 2.04$ , the amplitude of the scalar power spectrum  $P_S$  and the scalar spectral tilt  $n_S$  match the Planck 2015 data and also consistent with the joint constraint obtained from Planck+BICEP2+Keck Array. But in this regime the value of tensor-to-scalar ratio  $r$  exceeds the upper bound i.e.  $r > 0.12$ . On the other hand, for very low  $\beta$  the estimated value of the magnetic field at the present epoch  $B_0$  from the hilltop model is very very small and can be able to reach up to the lower bound  $B_0 > 10^{-15}$  Gauss. Similarly for low  $\beta$ , the reheating energy density  $\rho_{reh}$  or equivalently the reheating temperature  $T_{reh}$  falls down and also the rescaled reheating parameter  $R_{sc}$  decrease.
- For  $\beta > 2.4$ , the amplitude of the scalar power spectrum  $P_S$  and the scalar spectral tilt  $n_S$  are perfectly consistent with the Planck 2015 data and also consistent with the joint constraint obtained from Planck+BICEP2+Keck Array. But in this case the value of tensor-to-scalar ratio  $r$  is very very small compared to its the upper bound i.e.  $r \ll 0.12$ . As  $\beta$  increases the estimated value of the magnetic field at the present epoch  $B_0$  exceeds the upper bound i.e.  $B_0 \gg 10^{-9}$  Gauss as obtained from Faraday rotation. Additionally in the large  $\beta$  regime the reheating energy density  $\rho_{reh}$  or equivalently the reheating temperature  $T_{reh}$  and the rescaled reheating parameter  $R_{sc}$  are not consistent with the observational constraints.

## 7 Summary

To summarize, in the present article, I have established a theoretical constraint relationship on inflationary magnetogenesis in the framework of Randall-Sundrum braneworld gravity (RSII) from: (1) tensor-to-scalar ratio ( $r$ ), (2) reheating, (3) leptogenesis and (4) baryogenesis for a generic large and small field model of inflation with a flat potential, where inflation is driven by slow-roll. For such a class of model it is also possible to

predict amount of magnetic field at the present epoch ( $B_0$ ) by measuring non-vanishing CP asymmetry ( $\epsilon_{CP}$ ) in leptogenesis and baryon asymmetry ( $\eta_B$ ) in baryogenesis or the tensor-to-scalar ratio in the inflationary setup. Most significantly, once the signature of primordial gravity waves will be predicted by in any near future observational probes, it will be possible to comment on the associated CP asymmetry and baryon asymmetry and vice versa. In this paper I have used important cosmoparticle constraints arising from Planck on the amplitude of scalar power spectrum, scalar spectral tilt, the upper bound on tensor to scalar ratio, lower bound on rescaled characteristic reheating parameter and the bound on the reheating energy density within  $1.5\sigma - 2\sigma$  statistical CL. Further assuming the conformal invariance to be restored after inflation in the framework of Randall-Sundrum single braneworld gravity (RSII), I have explicitly shown that the requirement of the sub-dominant feature of large scale magnetic field after inflation gives two fold non-trivial characteristic constraints- on equation of state parameter ( $w$ ) and the corresponding energy scale during reheating ( $\rho_{rh}^{1/4}$ ) epoch. Hence avoiding the contribution of back-reaction from the magnetic field I have established a bound on the reheating characteristic parameter ( $R_{rh}$ ) and its rescaled version ( $R_{sc}$ ), to achieve large scale magnetic field within the prescribed setup and apply the Cosmic Microwave Background (CMB) constraints as obtained from recent Planck 2015 data. To this end I have explicitly shown the cosmophenomenological consequences from two specific models of brane inflation- monomial (large field) and hilltop (small field) after applying all the constraints obtained from “braneinflamagnetogenesis”. For monomial models of braneinflamagnetogenesis I get,  $5.969 \times 10^{-10}$  Gauss  $< B_0 < 4.638 \times 10^{-9}$  Gauss,  $4.061 \times 10^{-5} M_p^4 < \rho_{reh} < 1.591 \times 10^{-3} M_p^4$ ,  $1.940 \times 10^{-132} M_p^4 < \rho_{B_0} < 1.171 \times 10^{-130} M_p^4$ ,  $6.227 \times 10^{-4} \times g_*^{-1/4} M_p < T_{reh} < 4.836 \times 10^{-3} \times g_*^{-1/4} M_p$ ,  $\Gamma_{total} \sim 0.24 M_p$ ,  $1.55 \times 10^{-3} < R_{sc} < 1.24 \times 10^{-2}$ ,  $\epsilon_{CP} \sim \mathcal{O}(10^{-6})$ ,  $\eta_B \sim \mathcal{O}(10^{-9})$ ,  $0.121 < r < 0.124$ ,  $0.969 < n_S < 0.970$ ,  $2.3794 \times 10^{-9} < P_S < 2.3798 \times 10^{-9}$ ,  $8.08 \times 10^{-3} M_p < \sqrt[4]{V_0} < 8.13 \times 10^{-3} M_p$  for  $0.7 < \beta < 1.1$ ,  $-0.48 < \bar{w}_{reh} < -0.29$ ,  $\Delta\mathcal{N}_b = 50$ ,  $\Delta\tilde{\mathcal{N}}_b = 7$  and  $\sigma \sim 5 \times 10^{-16} M_p^4$ . Similarly for hilltop models of braneinflamagnetogenesis I get,  $1.238 \times 10^{-9}$  Gauss  $< B_0 < 1.263 \times 10^{-9}$  Gauss,  $4.945 \times 10^{-14} M_p^4 < \rho_{reh} < 5.128 \times 10^{-14} M_p^4$ ,  $8.345 \times 10^{-132} M_p^4 < \rho_{B_0} < 8.685 \times 10^{-132} M_p^4$ ,  $6.227 \times 10^{-4} \times g_*^{-1/4} M_p < T_{reh} < 6.283 \times 10^{-4} \times g_*^{-1/4} M_p$ ,  $\Gamma_{total} \sim 1.7 \times 10^{-4} M_p$ ,  $7 \times 10^{-5} < R_{sc} < 7.11 \times 10^{-5}$ ,  $\epsilon_{CP} \sim \mathcal{O}(10^{-6})$ ,  $\eta_B \sim \mathcal{O}(10^{-9})$ ,  $0.121 < r < 0.124$ ,  $0.969 < n_S < 0.970$ ,  $2.3794 \times 10^{-9} < P_S < 2.3798 \times 10^{-9}$ ,  $8.08 \times 10^{-3} M_p < \sqrt[4]{V_0} < 8.13 \times 10^{-3} M_p$  for  $2.04 < \beta < 2.4$ ,  $\bar{w}_{reh} = 0$ ,  $\Delta\mathcal{N}_b = 50$ ,  $\Delta\tilde{\mathcal{N}}_b = 11.5$ ,  $\sigma \sim 10^{-9} M_p^4$  and  $\mu = 1 M_p$ . The prescribed analysis performed in this paper also shows that the estimated cosmo-phenomenological parameters for both of the models of braneinflamagnetogenesis confronts well with the Planck 2015 data and Planck+BICEP2+Keck Array joint constraint within  $2\sigma$  CL for restricted choice of the parameter space of the model parameters within the framework of Randall-Sundrum single braneworld. Also it is important mention here that by doing parameter estimation from both of these simple class of models, it is clearly observed that the magneto-reheating constraints serve the purpose of breaking the degeneracy between the inflationary observables estimated from both of these inflationary models.

Further my aim is to carry forward this work in a more broader sense, where I will



apply all the derived results to the rest of the inflationary models within RSII setup. The other promising future prospects of this work are-

1. One can follow the prescribed methodology to derive the cosmophenomenological constraints in the context of various modified gravity framework i.e. Dvali-Gabadadze-Porrati (DGP) braneworld [68], Einstein-Hilbert-Gauss-Bonnet (EHGB) gravity [34, 69], Einstein-Gauss-Bonnet-Dilaton (EGBD) gravity [32, 33, 35, 36] and  $f(R)$  theory of gravity [71, 72] etc.
2. Hence using the derived constraints one can constrain various classes of large and small field inflationary models [66, 74, 75, 75, 77–80] within the framework of other modified theories of gravity.
3. One can explore various hidden cosmophenomenological features of CMB E-mode and B-mode polarization spectra from the various modified gravity frameworks, which can be treated as a significant probe to put further stringent constraint on various classes of large and small field inflationary models.
4. One can also study the model independent prescription of magnetogenesis by reconstructing inflationary potential from various cosmoparticle constraints from the observed data.

## Acknowledgments

I would like to thank Department of Theoretical Physics, Tata Institute of Fundamental Research, Mumbai for providing me Visiting (Post-Doctoral) Research Fellowship. I take this opportunity to thank sincerely to Prof. Soumitra SenGupta, Prof. Sayan Kar, Prof. Sandip P. Trivedi, Dr. Subhabrata Majumdar and Dr. Supratik Pal for their constant support and inspiration.

## 8 Appendix

### 8.1 Inflationary consistency relations in RSII

In the context of RSII the spectral tilts ( $n_S, n_T$ ), running of the tilts ( $\alpha_S, \alpha_T$ ) and running of the running of tilts ( $\kappa_T, \kappa_S$ ) at the momentum pivot scale  $k_*$  can be expressed as:

$$n_S(k_*) - 1 = 2\eta_b(\phi_*) - 6\epsilon_b(k_*), \quad (8.1)$$

$$n_T(k_*) = -3\epsilon_b(k_*) = -\frac{r(k_*)}{8}, \quad (8.2)$$

$$\alpha_S(k_*) = 16\eta_b(k_*)\epsilon_b(k_*) - 18\epsilon_b^2(k_*) - 2\xi_b^2(k_*), \quad (8.3)$$

$$\alpha_T(k_*) = 6\eta_b(k_*)\epsilon_b(k_*) - 9\epsilon_b^2(k_*), \quad (8.4)$$

$$\begin{aligned} \kappa_S(k_*) = 152\eta_b(k_*)\epsilon_b^2(k_*) - 32\epsilon_b(k_*)\eta_b^2(k_*) - 108\epsilon_b^3(k_*) \\ - 24\xi_b^2(k_*)\epsilon_b(k_*) + 2\eta_b(k_*)\xi_b^2(k_*) + 2\sigma_b^3(k_*), \end{aligned} \quad (8.5)$$

$$\kappa_T(k_*) = 66\eta_b(k_*)\epsilon_b^2(k_*) - 12\epsilon_b(k_*)\eta_b^2(k_*) - 54\epsilon_b^3(k_*) - 6\epsilon_b(k_*)\xi_b^2(k_*). \quad (8.6)$$

In terms of slow-roll parameters in RSII setup one can also write the following sets of consistency conditions for brane inflation:

$$n_T(k_*) - n_S(k_*) + 1 = \left( \frac{d \ln r(k)}{d \ln k} \right)_* = \left[ \frac{r(k_*)}{8} - 2\eta_b(k_*) \right], \quad (8.7)$$

$$\alpha_T(k_*) - \alpha_S(k_*) = \left( \frac{d^2 \ln r(k)}{d \ln k^2} \right)_* = \left[ \left( \frac{r(k_*)}{8} \right)^2 - \frac{20}{3} \left( \frac{r(k_*)}{8} \right) + 2\xi_b^2(k_*) \right], \quad (8.8)$$

$$\begin{aligned} \kappa_T(k_*) - \kappa_S(k_*) &= \left( \frac{d^3 \ln r(k)}{d \ln k^3} \right)_* \\ &= \left[ 2 \left( \frac{r(k_*)}{8} \right)^3 - \frac{86}{9} \left( \frac{r(k_*)}{8} \right)^2 \right. \\ &\quad \left. + \frac{4}{3} (6\xi_b^2(k_*) + 5\eta_b^2(k_*)) \left( \frac{r(k_*)}{8} \right) + 2\eta_b(k_*)\xi_b^2(k_*) + 2\sigma_b^3(k_*) \right]. \end{aligned} \quad (8.9)$$

Here Eq (8.7-8.9) represent the running, running of the running and running of the double running of tensor-to-scalar ratio in RSII brane inflationary setup. Within high energy limit  $\rho \gg \sigma$  the slow-roll parameters in the visible brane can be expressed as:

$$\epsilon_b(\phi) \approx \frac{2M_p^2 \sigma (V'(\phi))^2}{V^3(\phi)}, \quad (8.10)$$

$$\eta_b(\phi) \approx \frac{2M_p^2 \sigma V''(\phi)}{V^2(\phi)}, \quad (8.11)$$

$$\xi_b^2(\phi) \approx \frac{4M_p^4 \sigma^2 V'(\phi) V'''(\phi)}{V^4(\phi)}, \quad (8.12)$$

$$\sigma_b^3(\phi) \approx \frac{8M_p^6 \sigma^3 (V'(\phi))^2 V''''(\phi)}{V^6(\phi)}. \quad (8.13)$$

and consequently the number of e-foldings can be written as:

$$\Delta \mathcal{N}_b = \mathcal{N}_b(\phi_{cmb}) - \mathcal{N}_b(\phi_e) \approx \frac{1}{2\sigma M_p^2} \int_{\phi_e}^{\phi_{cmb}} d\phi \frac{V^2(\phi)}{V'(\phi)} \quad (8.14)$$

where  $\phi_e$  corresponds to the field value at the end of inflation, which can be obtained from the following constraint equation:

$$\max_{\phi=\phi_e} [\epsilon_b, |\eta_b|, |\xi_b^2|, |\sigma_b^3|] = 1. \quad (8.15)$$

## 8.2 Evaluation of $I_\xi(k_L, k_\Lambda)$ integral kernel

$$I_\xi(k_L; k_\Lambda) = \begin{cases} \frac{\sqrt{\pi}}{2\xi k_*} [\text{erf}(\xi k_\Lambda) - \text{erf}(\xi k_L)] & \text{for Case I} \\ \frac{1}{2(\xi k_*)^{n_B+3}} \left[ \Gamma\left(\frac{(n_B+3)}{2}, \xi^2 k_L^2\right) - \Gamma\left(\frac{(n_B+3)}{2}, \xi^2 k_\Lambda^2\right) \right] & \text{for Case II} \\ \left[ \frac{\sqrt{\pi}}{2\xi k_*} \text{erf}(\xi k) \left\{ 1 + \mathcal{Q} \ln\left(\frac{k}{k_*}\right) + \mathcal{P} \ln^2\left(\frac{k}{k_*}\right) \right\} \right. \\ \quad + \left(\frac{k}{k_*}\right) \left\{ 2\mathcal{P} {}_P F_Q \left[ \left\{ \frac{1}{2}, \frac{1}{2}, \frac{1}{2} \right\} ; \left\{ \frac{3}{2}, \frac{3}{2}, \frac{3}{2} \right\} ; -\xi^2 k^2 \right] \right. \\ \quad \left. \left. - \left( \mathcal{Q} + 2\mathcal{P} \ln\left(\frac{k}{k_*}\right) \right) {}_P F_Q \left[ \left\{ \frac{1}{2}, \frac{1}{2} \right\} ; \left\{ \frac{3}{2}, \frac{3}{2} \right\} ; -\xi^2 k^2 \right] \right\} \right]_{k=k_L}^{k=k_\Lambda} & \text{for Case III} \\ \left[ \frac{\sqrt{\pi}}{2\xi k_*} \text{erf}(\xi k) \left\{ 1 + \mathcal{Q} \ln\left(\frac{k}{k_*}\right) + \mathcal{P} \ln^2\left(\frac{k}{k_*}\right) + \mathcal{F} \ln^3\left(\frac{k}{k_*}\right) \right\} \right. \\ \quad + \left(\frac{k}{k_*}\right) \left\{ -6\mathcal{F} {}_P F_Q \left[ \left\{ \frac{1}{2}, \frac{1}{2}, \frac{1}{2}, \frac{1}{2} \right\} ; \left\{ \frac{3}{2}, \frac{3}{2}, \frac{3}{2}, \frac{3}{2} \right\} ; -\xi^2 k^2 \right] \right. \\ \quad + 2 \left( \mathcal{P} + 3\mathcal{F} \ln\left(\frac{k}{k_*}\right) \right) {}_P F_Q \left[ \left\{ \frac{1}{2}, \frac{1}{2}, \frac{1}{2} \right\} ; \left\{ \frac{3}{2}, \frac{3}{2}, \frac{3}{2} \right\} ; -\xi^2 k^2 \right] \\ \quad \left. \left. - \left( \mathcal{Q} + 2\mathcal{P} \ln\left(\frac{k}{k_*}\right) + 6\mathcal{F} \ln^2\left(\frac{k}{k_*}\right) \right) \right. \right. \\ \quad \left. \left. \times {}_P F_Q \left[ \left\{ \frac{1}{2}, \frac{1}{2} \right\} ; \left\{ \frac{3}{2}, \frac{3}{2} \right\} ; -\xi^2 k^2 \right] \right\} \right]_{k=k_L}^{k=k_\Lambda} & \text{for Case IV} \end{cases} \quad (8.16)$$

where  $\mathcal{Q} = n_B + 2$ ,  $\mathcal{P} = \alpha_B/2$  and  $\mathcal{F} = \kappa_B/6$ .

## 8.3 Evaluation of $J(k_L, k_\Lambda)$ integral kernel

$$J(k_L; k_\Lambda) = \begin{cases} \frac{1}{3} \left[ \left(\frac{k_\Lambda}{k_*}\right)^3 - \left(\frac{k_L}{k_*}\right)^3 \right] & \text{for Case I} \\ \frac{1}{(n_B+3)} \left[ \left(\frac{k_\Lambda}{k_*}\right)^{n_B+3} - \left(\frac{k_L}{k_*}\right)^{n_B+3} \right] & \text{for Case II} \\ \left\{ \left(\frac{k}{k_*}\right) \left[ (1 + 2\mathcal{P} - \mathcal{Q}) + (\mathcal{Q} - 2\mathcal{P}) \ln\left(\frac{k}{k_*}\right) + \mathcal{P} \ln^2\left(\frac{k}{k_*}\right) \right] \right\}_{k=k_L}^{k=k_\Lambda} & \text{for Case III} \\ \left\{ \left(\frac{k}{k_*}\right) \left[ (1 - 6\mathcal{F} + 2\mathcal{P} - \mathcal{Q}) + (6\mathcal{F} - 2\mathcal{P} + \mathcal{Q}) \ln\left(\frac{k}{k_*}\right) \right. \right. \\ \quad \left. \left. - (3\mathcal{F} - \mathcal{P}) \ln^2\left(\frac{k}{k_*}\right) + \mathcal{F} \ln^3\left(\frac{k}{k_*}\right) \right] \right\}_{k=k_L}^{k=k_\Lambda} & \text{for Case IV} \end{cases} \quad (8.17)$$

where  $\mathcal{Q} = n_B + 2$ ,  $\mathcal{P} = \alpha_B/2$  and  $\mathcal{F} = \kappa_B/6$ .

## References

- [1] K. T. Chyzy and R. Beck, “*Magnetic fields in merging spirals - The Antennae,*” *Astron. Astrophys.* **417** (2004) 541 [astro-ph/0401157].
- [2] C. Vogt and T. A. Ensslin, “*Measuring the cluster magnetic field power spectra from Faraday Rotation maps of Abell 400, Abell 2634 and Hydra A,*” *Astron. Astrophys.* **412** (2003) 373 [astro-ph/0309441].
- [3] D. Grasso and H. R. Rubinstein, “*Magnetic fields in the early universe,*” *Phys. Rept.* **348** (2001) 163 [astro-ph/0009061].
- [4] M. Giovannini, “*The Magnetized universe,*” *Int. J. Mod. Phys. D* **13** (2004) 391 [astro-ph/0312614].
- [5] A. Kandus, K. E. Kunze and C. G. Tsagas, “*Primordial magnetogenesis,*” *Phys. Rept.* **505** (2011) 1 [arXiv:1007.3891 [astro-ph.CO]].
- [6] R. Durrer and A. Neronov, “*Cosmological Magnetic Fields: Their Generation, Evolution and Observation,*” *Astron. Astrophys. Rev.* **21** (2013) 62 [arXiv:1303.7121 [astro-ph.CO]].
- [7] W. Essey, S. Ando and A. Kusenko, “*Determination of intergalactic magnetic fields from gamma ray data,*” *Astropart. Phys.* **35** (2011) 135 [arXiv:1012.5313 [astro-ph.HE]].
- [8] P. P. Kronberg, “*Extragalactic magnetic fields,*” *Rept. Prog. Phys.* **57** (1994) 325.
- [9] F. Tavecchio, G. Ghisellini, L. Foschini, G. Bonnoli, G. Ghirlanda and P. Coppi, “*The intergalactic magnetic field constrained by Fermi/LAT observations of the TeV blazar 1ES 0229+200,*” *Mon. Not. Roy. Astron. Soc.* **406** (2010) L70 [arXiv:1004.1329 [astro-ph.CO]].
- [10] A. Neronov and I. Vovk, “*Evidence for strong extragalactic magnetic fields from Fermi observations of TeV blazars,*” *Science* **328** (2010) 73 [arXiv:1006.3504 [astro-ph.HE]].
- [11] K. Dolag, M. Kachelriess, S. Ostapchenko and R. Tomas, “*Lower limit on the strength and filling factor of extragalactic magnetic fields,*” *Astrophys. J.* **727** (2011) L4 [arXiv:1009.1782 [astro-ph.HE]].
- [12] M. S. Turner and L. M. Widrow, “*Inflation Produced, Large Scale Magnetic Fields,*” *Phys. Rev. D* **37** (1988) 2743.
- [13] B. Ratra, “*Cosmological ‘seed’ magnetic field from inflation,*” *Astrophys. J.* **391** (1992) L1.
- [14] A. Dolgov and J. Silk, “*Electric charge asymmetry of the universe and magnetic field generation,*” *Phys. Rev. D* **47** (1993) 3144.
- [15] A. Dolgov, “*Breaking of conformal invariance and electromagnetic field generation in the universe,*” *Phys. Rev. D* **48** (1993) 2499 [hep-ph/9301280].
- [16] B. Ratra and P. J. E. Peebles, “*Inflation in an open universe,*” *Phys. Rev. D* **52** (1995) 1837.
- [17] O. Tornkvist, A. C. Davis, K. Dimopoulos and T. Prokopec, “*Large scale primordial magnetic fields from inflation and preheating,*” *AIP Conf. Proc.* **555** (2001) 443 [astro-ph/0011278].
- [18] K. Subramanian, “*The origin, evolution and signatures of primordial magnetic fields,*”

arXiv:1504.02311 [astro-ph.CO].

- [19] K. Atmjeet, I. Pahwa, T. R. Seshadri and K. Subramanian, “*Cosmological Magnetogenesis From Extra-dimensional Gauss Bonnet Gravity*,” *Phys. Rev. D* **89** (2014) 6, 063002 [arXiv:1312.5815 [astro-ph.CO]].
- [20] K. Atmjeet, T. R. Seshadri and K. Subramanian, “*Helical cosmological magnetic fields from extra-dimensions*,” arXiv:1409.6840 [astro-ph.CO].
- [21] K. Subramanian, “*Magnetic fields in the early universe*,” *Astron. Nachr.* **331** (2010) 110 [arXiv:0911.4771 [astro-ph.CO]].
- [22] C. T. Byrnes, L. Hollenstein, R. K. Jain and F. R. Urban, “*Resonant magnetic fields from inflation*,” *JCAP* **1203** (2012) 009 [arXiv:1111.2030 [astro-ph.CO]].
- [23] R. J. Z. Ferreira, R. K. Jain and M. S. Sloth, “*Inflationary magnetogenesis without the strong coupling problem*,” *JCAP* **1310** (2013) 004 [arXiv:1305.7151 [astro-ph.CO]].
- [24] R. J. Z. Ferreira, R. K. Jain and M. S. Sloth, “*Inflationary Magnetogenesis without the Strong Coupling Problem II: Constraints from CMB anisotropies and B-modes*,” *JCAP* **1406** (2014) 053 [arXiv:1403.5516 [astro-ph.CO]].
- [25] R. K. Jain and M. S. Sloth, “*Consistency relation for cosmic magnetic fields*,” *Phys. Rev. D* **86** (2012) 123528 [arXiv:1207.4187 [astro-ph.CO]].
- [26] L. Randall and R. Sundrum, “*A Large mass hierarchy from a small extra dimension*,” *Phys. Rev. Lett.* **83** (1999) 3370 [hep-ph/9905221].
- [27] L. Randall and R. Sundrum, “*An Alternative to compactification*,” *Phys. Rev. Lett.* **83** (1999) 4690 [hep-th/9906064].
- [28] S. Choudhury and S. Pal, “*Brane inflation in background supergravity*,” *Phys. Rev. D* **85** (2012) 043529 [arXiv:1102.4206 [hep-th]].
- [29] S. Choudhury and S. Pal, “*Reheating and leptogenesis in a SUGRA inspired brane inflation*,” *Nucl. Phys. B* **857** (2012) 85 [arXiv:1108.5676 [hep-ph]].
- [30] S. Choudhury and S. Pal, “*Brane inflation: A field theory approach in background supergravity*,” *J. Phys. Conf. Ser.* **405** (2012) 012009 [arXiv:1209.5883 [hep-th]].
- [31] S. Choudhury, “*Can Effective Field Theory of inflation generate large tensor-to-scalar ratio within Randall-Sundrum single braneworld?*,” *Nucl. Phys. B* **894** (2015) 29 [arXiv:1406.7618 [hep-th]].
- [32] S. Choudhury and S. SenGupta, “*Features of warped geometry in presence of Gauss-Bonnet coupling*,” *JHEP* **1302** (2013) 136 [arXiv:1301.0918 [hep-th]].
- [33] S. Choudhury and S. SenGupta, “*A step toward exploring the features of Gravidilaton sector in Randall-Sundrum scenario via lightest Kaluza-Klein graviton mass*,” *Eur. Phys. J. C* **74** (2014) 11, 3159 [arXiv:1311.0730 [hep-ph]].
- [34] S. Choudhury, S. Sadhukhan and S. SenGupta, “*Collider constraints on Gauss-Bonnet coupling in warped geometry model*,” arXiv:1308.1477 [hep-ph].
- [35] S. Choudhury, J. Mitra and S. SenGupta, “*Modulus stabilization in higher curvature dilaton gravity*,” *JHEP* **1408** (2014) 004 [arXiv:1405.6826 [hep-th]].
- [36] S. Choudhury, J. Mitra and S. SenGupta, “*Fermion localization and flavour hierarchy*

- in higher curvature spacetime*,” arXiv:1503.07287 [hep-th].
- [37] Y. Himemoto and M. Sasaki, “*Brane world inflation without inflaton on the brane*,” Phys. Rev. D **63** (2001) 044015 [gr-qc/0010035].
  - [38] B. Mukhopadhyaya, S. Sen and S. SenGupta, “*Does a Randall-Sundrum scenario create the illusion of a torsion free universe?*,” Phys. Rev. Lett. **89** (2002) 121101 [Phys. Rev. Lett. **89** (2002) 259902] [hep-th/0204242].
  - [39] R. Maartens and K. Koyama, “*Brane-World Gravity*,” Living Rev. Rel. **13** (2010) 5 [arXiv:1004.3962 [hep-th]].
  - [40] P. Brax, C. van de Bruck and A. C. Davis, “*Brane world cosmology*,” Rept. Prog. Phys. **67** (2004) 2183 [hep-th/0404011].
  - [41] C. S. Fong, E. Nardi and A. Riotto, “*Leptogenesis in the Universe*,” Adv. High Energy Phys. **2012** (2012) 158303 [arXiv:1301.3062 [hep-ph]].
  - [42] S. Davidson, E. Nardi and Y. Nir, “*Leptogenesis*,” Phys. Rept. **466** (2008) 105 [arXiv:0802.2962 [hep-ph]].
  - [43] W. Buchmuller, R. D. Peccei and T. Yanagida, “*Leptogenesis as the origin of matter*,” Ann. Rev. Nucl. Part. Sci. **55** (2005) 311 [hep-ph/0502169].
  - [44] D. E. Morrissey and M. J. Ramsey-Musolf, “*Electroweak baryogenesis*,” New J. Phys. **14** (2012) 125003 [arXiv:1206.2942 [hep-ph]].
  - [45] M. Trodden, “*Electroweak baryogenesis*,” Rev. Mod. Phys. **71** (1999) 1463 [hep-ph/9803479].
  - [46] J. M. Cline, “*Baryogenesis*,” arXiv:hep-ph/0609145.
  - [47] R. Allahverdi and A. Mazumdar, “*A mini review on Affleck-Dine baryogenesis*,” New J. Phys. **14** (2012) 125013.
  - [48] P. A. R. Ade *et al.* [Planck Collaboration], “*Planck 2015 results. XIX. Constraints on primordial magnetic fields*,” arXiv:1502.01594 [astro-ph.CO].
  - [49] P. A. R. Ade *et al.* [Planck Collaboration], “*Planck 2015 results. XIII. Cosmological parameters*,” arXiv:1502.01589 [astro-ph.CO].
  - [50] P. A. R. Ade *et al.* [Planck Collaboration], “*Planck 2015 results. XX. Constraints on inflation*,” arXiv:1502.02114 [astro-ph.CO].
  - [51] P. A. R. Ade *et al.* [BICEP2 and Planck Collaborations], arXiv:1502.00612 [astro-ph.CO].
  - [52] M. Shiraishi, D. Nitta, S. Yokoyama, K. Ichiki and K. Takahashi, “*CMB Bispectrum from Primordial Scalar, Vector and Tensor non-Gaussianities*,” Prog. Theor. Phys. **125** (2011) 795 [arXiv:1012.1079 [astro-ph.CO]].
  - [53] M. Shiraishi, D. Nitta, S. Yokoyama and K. Ichiki, “*Optimal limits on primordial magnetic fields from CMB temperature bispectrum of passive modes*,” JCAP **1203** (2012) 041 [arXiv:1201.0376 [astro-ph.CO]].
  - [54] S. Choudhury, “*Inflamagnetogenesis redux: Unzipping sub-Planckian inflation via various cosmoparticle probes*,” Phys. Lett. B **735** (2014) 138 [arXiv:1403.0676 [hep-th]].
  - [55] A. J. Long, E. Sabancilar and T. Vachaspati, “*Leptogenesis and Primordial Magnetic*

- Fields*,” JCAP **1402** (2014) 036 [arXiv:1309.2315 [astro-ph.CO]].
- [56] M. Fukugita and T. Yanagida, “*Baryogenesis Without Grand Unification*,” Phys. Lett. B **174** (1986) 45.
- [57] W. Buchmuller, R. D. Peccei and T. Yanagida, “*Leptogenesis as the origin of matter*,” Ann. Rev. Nucl. Part. Sci. **55** (2005) 311 [hep-ph/0502169].
- [58] I. Agullo and J. Navarro-Salas, “*Conformal anomaly and primordial magnetic fields*,” arXiv:1309.3435 [gr-qc].
- [59] V. Demozzi and C. Ringeval, “*Reheating constraints in inflationary magnetogenesis*,” JCAP **1205** (2012) 009 [arXiv:1202.3022 [astro-ph.CO]].
- [60] S. Choudhury and A. Mazumdar, “*Reconstructing inflationary potential from BICEP2 and running of tensor modes*,” arXiv:1403.5549 [hep-th].
- [61] S. Choudhury and A. Mazumdar, “*Sub-Planckian inflation & large tensor to scalar ratio with  $r \geq 0.1$* ,” arXiv:1404.3398 [hep-th].
- [62] S. Choudhury and A. Mazumdar, “*An accurate bound on tensor-to-scalar ratio and the scale of inflation*,” Nucl. Phys. B **882** (2014) 386 [arXiv:1306.4496 [hep-ph]].
- [63] S. Choudhury, A. Mazumdar and S. Pal, “*Low & High scale MSSM inflation, gravitational waves and constraints from Planck*,” JCAP **1307** (2013) 041 [arXiv:1305.6398 [hep-ph]].
- [64] S. Choudhury and A. Mazumdar, “*Primordial blackholes and gravitational waves for an inflection-point model of inflation*,” Phys. Lett. B **733** (2014) 270 [arXiv:1307.5119 [astro-ph.CO]].
- [65] S. Choudhury and S. Pal, “*Fourth level MSSM inflation from new flat directions*,” JCAP **1204** (2012) 018 [arXiv:1111.3441 [hep-ph]].
- [66] A. Mazumdar and J. Rocher, “*Particle physics models of inflation and curvaton scenarios*,” Phys. Rept. **497** (2011) 85 [arXiv:1001.0993 [hep-ph]].
- [67] P. A. R. Ade *et al.* [Planck Collaboration], Astron. Astrophys. **571** (2014) A22 [arXiv:1303.5082 [astro-ph.CO]].
- [68] G. R. Dvali, G. Gabadadze and M. Porrati, “*4-D gravity on a brane in 5-D Minkowski space*,” Phys. Lett. B **485** (2000) 208 [hep-th/0005016].
- [69] U. Maitra, B. Mukhopadhyaya and S. SenGupta, “*Reconciling small radion vacuum expectation values with massive gravitons in an Einstein-Gauss-Bonnet warped geometry scenario*,” arXiv:1307.3018.
- [70] S. Choudhury and S. SenGupta, “*Thermodynamics of Charged Kalb Ramond AdS black hole in presence of Gauss-Bonnet coupling*,” arXiv:1306.0492 [hep-th].
- [71] A. De Felice and S. Tsujikawa, “*f(R) theories*,” Living Rev. Rel. **13** (2010) 3 [arXiv:1002.4928 [gr-qc]].
- [72] T. P. Sotiriou and V. Faraoni, “*f(R) Theories Of Gravity*,” Rev. Mod. Phys. **82** (2010) 451 [arXiv:0805.1726 [gr-qc]].
- [73] J. Martin and C. Ringeval, “*First CMB Constraints on the Inflationary Reheating Temperature*,” Phys. Rev. D **82** (2010) 023511 [arXiv:1004.5525 [astro-ph.CO]].

- [74] J. Martin, C. Ringeval and V. Vennin, “*Encyclopdia Inflationaris*,” *Phys. Dark Univ.* (2014) [arXiv:1303.3787 [astro-ph.CO]].
- [75] J. Martin, C. Ringeval and V. Vennin, “*How Well Can Future CMB Missions Constrain Cosmic Inflation?*,” *JCAP* **1410** (2014) 10, 038 [arXiv:1407.4034 [astro-ph.CO]].
- [76] J. Martin, C. Ringeval, R. Trotta and V. Vennin, “*Compatibility of Planck and BICEP2 in the Light of Inflation*,” *Phys. Rev. D* **90** (2014) 6, 063501 [arXiv:1405.7272 [astro-ph.CO]].
- [77] J. Martin, C. Ringeval, R. Trotta and V. Vennin, “*The Best Inflationary Models After Planck*,” *JCAP* **1403** (2014) 039 [arXiv:1312.3529 [astro-ph.CO]].
- [78] A. Linde, “*Inflationary Cosmology after Planck 2013*,” arXiv:1402.0526 [hep-th].
- [79] D. H. Lyth and A. Riotto, “*Particle physics models of inflation and the cosmological density perturbation*,” *Phys. Rept.* **314** (1999) 1 [hep-ph/9807278].
- [80] D. H. Lyth, “*Particle physics models of inflation*,” *Lect. Notes Phys.* **738** (2008) 81 [hep-th/0702128].